A holistic approach to risk-based decision on inspection and design of fatigue-sensitive structures

Guang Zou[a,b], Michael H. Faber[c], Arturo González[b], Kian Banisoleiman[a]
[a]Lloyd's Register Global Technology Centre, Lloyd's Register Group Limited, Southampton, UK
[b]School of Civil Engineering, University College Dublin, Dublin, Ireland
[c]Department of Civil Engineering, Aalborg University, Aalborg, Denmark

Key words: Structural management; Probabilistic optimization; Risk analysis; Risk-based inspection; Life cycle engineering; Decision analysis

Abstract

Design and operation of large welded structural systems (e.g. ship and offshore structures) are challenging due to numerous fatigue-sensitive details, limited available budgets, uncertainties in fatigue damages, inspection & maintenance activities, etc. Traditionally, fatigue design and maintenance planning have been almost disconnected, which restricts coherent decision-making and optimum safety management. Structural design optimization, without quantitatively incorporating the effects of operational maintenance, can hardly result in a structural plan that is optimum in terms of life cycle costs. Also, if the design of a structure is not optimum, maintenance optimization alone cannot yield a really optimum maintenance plan. As operational inspections and maintenance are essential, there are merits to utilize their effects to structural design and meanwhile optimize them at the initial design stage when impacts of decisions are greater. This paper proposes a risk-based approach to holistic decision-making enveloping decisions and uncertainties affecting design, inspection and maintenance of fatigue-sensitive components. Decisions variables in structural scantling and operational maintenance are obtained holistically at the structural design stage by risk based optimization, based on quantitative assessment of the effectiveness of both structural scantling and maintenance interventions. Optimum fatigue reliability level is also obtained, informed by the effects of uncertainties and failure consequences. The method captures combined benefits of structural scantling and operational maintenance to fatigue reliability and risk mitigation and achieves optimum resource utilization and life cycle cost reduction. Advantages of the proposed method have been demonstrated via a numerical example, In comparison to alternative methods.

1 Introduction

Fatigue deterioration, which leads to structural integrity loss in the form of crack initiation and propagation, is a common phenomenon in welded structural systems under cyclic loading (e.g. ship and offshore structures). Cracks typically initiate at local stress concentration areas or at welded details containing initial flaws, and then propagate quickly under sustained stress cycles. Crack propagation can lead to fracture of structural components and sudden failure of the whole structural system, e.g. rupture and cross section failure of ships, cracking of a leg causing collapse of an offshore platform, etc. These failures are often catastrophic, causing significant financial, social and environmental losses. Hence, the design and operation of welded structural systems is associated with high risks from fatigue failures.

Fatigue-sensitive components are designed traditionally by a S-N method, aiming to ensure a predicted fatigue life longer than required service life. S-N curves give fatigue life under a given stress range. Based on a fatigue design factor (FDF) and required service life, an allowable stress range can be obtained based on a S-N curve.

Nevertheless, in engineering practice fatigue cracks have been found common in large welded structures after several years' service. From a practical perspective, fatigue resistance is highly sensitive to factors such as initial imperfects in materials, residual stresses, welding notches, etc., and these factors are only partly controllable and have not been adequately accounted for by S-N curves. Moreover, there are modelling uncertainties associated with both fatigue capacity and fatigue loading calculation methods. It is typically not economical trying to avoid fatigue cracking by design measures only, in view of the significant costs needed to counteract the uncertainties [1, 2].

In fact, operational inspections are often essential for timely detection of fatigue cracks and detection of gross design errors, over loading, abnormal vibration, etc. [3]. It is thus sensible to quantify and exploit the effects of operational inspections and maintenance at the design stage and address the fatigue cracking problem with a holistic decision-making approach to optimum allocation of risk mitigation measures and resources in the lifetime, e.g. measures at the design, construction and operation stage given by Figure 1. Important engineering decisions against fatigue cracking are structural scantlings, welding and quality assurance techniques, and inspection & maintenance plans. A limitation in current engineering practice possibly is that these decisions are typically made separately and sequentially (Figure 1), which restricts coherent decision-making and optimum safety management.

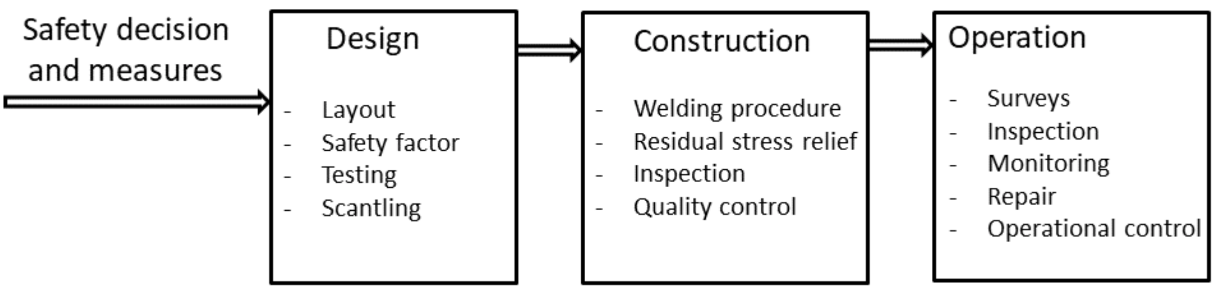

Figure 1: Lifetime safety decisions and measures against fatigue

Optimization of inspection & maintenance decisions can reduce operation costs, which can account for a significant part of life cycle costs of engineering structures with a large number of fatigue-sensitive details [3]. Optimal engineering decision-making is often challenged by limited data, knowledge and budgets. It is well-known that fatigue analysis is associated with a high degree of uncertainty. Many studies have been conducted to support engineering decisions against fatigue cracking, via analytical methods [4], experimental methods [5] and numerical methods [6]. S-N method has been widely adopted in designing structures against fatigue, including both deterministic design methods [7] and probabilistic design methods [8]. The fracture mechanics (FM) method has been used to develop probabilistic models to assess fatigue reliability [9-11], to update inspection plans [12-17], and to develop cost-effective inspection & maintenance plans for existing structures [1, 18-21]. The studies address almost exclusively either fatigue design issues with little quantitative analysis in operational maintenance or address maintenance issues based on given design plans or existing structures. There are needs to develop a holistic approach to quantify and utilize the combined benefits of design measures, inspections and maintenance to lifetime fatigue reliability and risk mitigation, in support of holistic optimization of these engineering activities subjected to associated uncertainties. In this regard, [22] develops a method to achieve the best trade-off between costs and safety for design and operation of pipelines against corrosion.
This paper provides a risk-based holistic decision-making (HDM) approach enveloping the design, inspection and maintenance decisions against fatigue cracking (Figure 2) and considering uncertainties and failure consequences affecting optimum decision-making. The optimum decision-making problem is addressed from an initial design perspective by risk-based structural optimization adopting major decision variables in structural scanting and maintenance planning (i.e. plate thickness and inspection intervals) as optimization variables. The

approach is an extension of risk-based design optimization by integration of maintenance optimization. A main feature of this approach is that fatigue design, inspection and maintenance decisions are optimized holistically, as opposed to separately, and thus the effectiveness of these risk mitigation measures is optimum utilized in the initial design decision-making process when the impacts of decisions are greater. As a result, the best trade-off between design (and construction) costs and maintenance costs can be achieved, contributing to a really optimum trade-off between safety and life cycle total costs. Another feature of the approach is that derived engineering decisions are based on the same risk model, and thus the decision-making process is coherent, and the expected lifetime fatigue reliability is trackable.

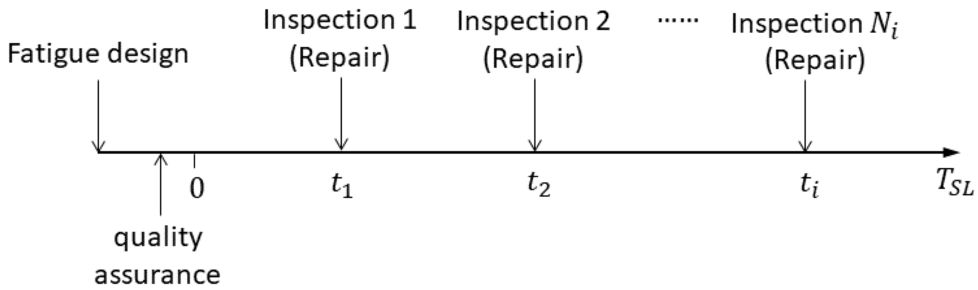

Figure 2: A schematically illustration of holistic decision-making against fatigue

This paper is organised as follows. Section 2 describes the probabilistic aspects of FM and S-N fatigue analysis methods. The proposed risk-based HDM method is developed based on probabilistic FM method, which is calibrated to S-N curves. Section 3 introduces the adopted maintenance strategy which relate repair decisions to inspection results. Section 4 presents a probabilistic inspection modelling approach and provides the probability of detection (PoD) curves for three inspection methods examined in this paper: magnetic particle inspection (MPI), close visual inspection (CVI) and visual inspection (VI). Section 5 formulates the risk-based HDM approach, integrating event tree analysis, reliability & risk quantification, life cycle analysis, and probabilistic optimization. Comparison approaches are also formulated: risk-based separate decision-making (SDM) method and reliability-based HDM method. A numerical example on ship structures is provided in Section 6, by which advantages of the proposed method are demonstrated. Section 7 summarizes the rationale, methodology and main conclusions.

2 Probabilistic fatigue analysis

Probabilistic FM method provides means of modelling the crack growth and associated uncertainties explicitly and allows for fatigue life and reliability/risk updating with inspection results by Bayesian Theorem. It also facilitates reliability and risk calculation, taking into account the effects of future inspections and repairs, and thus realization of inspection and repair optimization according to reliability & risk objectives. Therefore, the FM method is applied to fatigue deterioration modelling and to representation of effects of different fatigue design, inspection and maintenance plans in this paper. The probabilistic FM method is calibrated to S-N method using reliability index, which is also described in this section.

2.1 Probabilistic S-N method

S-N curves are derived from specimen experiments. Fatigue lives of different classes of structural details under different stress ranges and experimental conditions are analysed statistically. Then the relationship between fatigue life and stress range is established by a S-N curve, which represents the fatigue resistance of a specific class of structural details.

2.1.1 S-N curve

Equation 1 gives the formulation of a typical two-segment S-N curves adopted in marine engineering [7].

$$\begin{cases} N_F \Delta\sigma^{m_1} = \overline{a_1} & N_F \leq 10^7 \\ N_F \Delta\sigma^{m_2} = \overline{a_2} & N_F \geq 10^7 \end{cases} \tag{1}$$

Where $\Delta\sigma$ is stress range, N_F is fatigue life, m_1 and m_2 are the fatigue strength exponents, and $\overline{a_1}$ and $\overline{a_2}$ are the fatigue strength coefficients.

2.1.2 Fatigue loading

For marine & offshore structures, fatigue loads mainly come from waves. Some simplified calculation formulations, numerical methods, field measurements, as well as statistical counting methods have been developed to capture the stochastic natures of wave loading and structural responses [23-25]. It is generally acknowledged that the long-term distribution of stress ranges $\Delta\sigma$ can be modelled by a the two-parameter Weibull distribution as Equation 2 for simplified fatigue assessment with reasonable accuracy [14, 26, 27].

$$F(\Delta\sigma) = 1 - \exp\left[-\left(\frac{\Delta\sigma}{q}\right)^h\right] \tag{2}$$

where F is the cumulative probability function of $\Delta\sigma$, h is the Weibull shape parameter and q is the Weibull scale parameter.

2.1.3 Fatigue damage accumulation

Miner's rule [28], given by Equation (3), is widely used as an accumulation law for fatigue damage D. Uncertainty associated with Miner's rule is discussed by [26]. Some fatigue damage accumulation models are developed based on Miner's rule [29, 30], and a review on fatigue damage estimation models is provided by [31]

$$D = \sum_{i=1}^{n_b} \frac{n_i}{N_{fi}} \tag{3}$$

where n_i is number of load cycles at the i stress range level; N_{fi} is the fatigue capacity under the i stress range level; and n_b is the number of stress range levels.

Based on Equations (1) - (3), fatigue damage $D(t)$, given by Equation (4), can be obtained via Rainflow stress range counting. Detailed derivation is referred to [7].

$$D(t) = N_0 \cdot t \cdot \left[\frac{q^{m_1}}{\overline{a_1}} \Gamma\left(1 + \frac{m_1}{h};\ \left(\frac{S_1}{q}\right)^h\right) + \frac{q^{m_2}}{\overline{a_2}} \Upsilon\left(1 + \frac{m_2}{h};\ \left(\frac{S_1}{q}\right)^h\right)\right] \tag{4}$$

Where $D(t)$ is fatigue damage at time t, N_0 is the annual number of stress cycles, t is service year, Γ is the complementary incomplete Gamma function, Υ is the incomplete Gamma function and, S_1 is the transition stress range of two-segment S-N curve.

2.1.4 Fatigue reliability analysis

Equation (5) gives a limit state function, h_1, based on the S-N method.

$$h_1(t) = \Delta - D(t) \tag{5}$$

where Δ is fatigue damage at failure, i.e. the failure criterion, and D is given by Equation (4).
Even though the S-N approach is based on experimental data, there are still several sources of uncertainties. It is generally acknowledged that uncertainties come from both S-N data and Miner's rule. Uncertainties in fatigue failure criterion are discussed by [26, 32, 33]. The use of a bias of 1.0 and coefficient of variation (COV) of 0.3 are suggested for covering modelling error caused by Miner's rule [26]. Uncertainties associated with S-N data are normally indicated in design codes [7]. Figure 3 schematically shows the scatters in fatigue resistance.

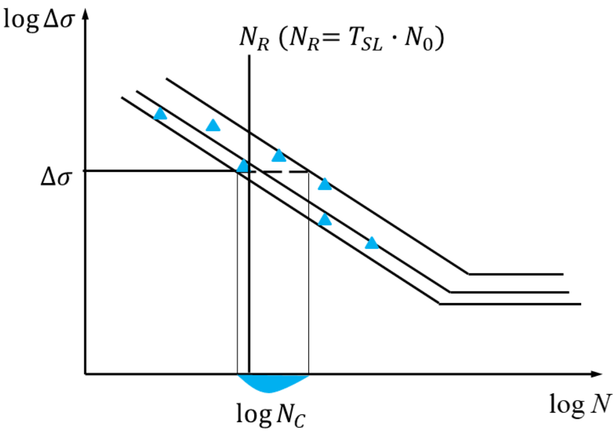

Figure 3: Illustration of fatigue resistance with the S-N method (T_{SL} is required service life in years, N_R is required number of cycles)

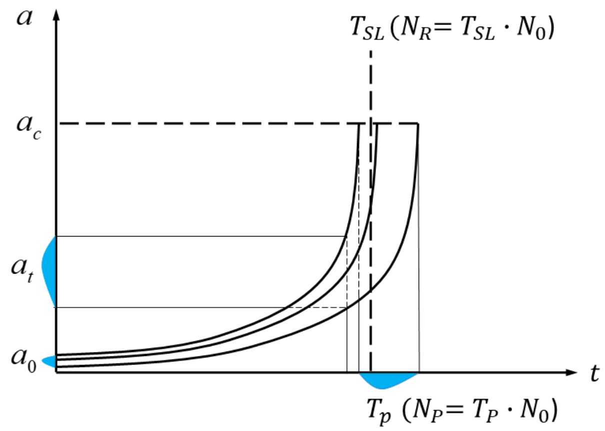

Figure 4: Illustration of fatigue resistance with the fracture mechanics (FM) method (T_P is crack propagation time in years)

Equations (6) and (7) give the failure probability $p_{f,SN}(t)$ and reliability index $\beta_{SN}(t)$ based on S-N method, where $\Phi^{-1}[\cdot]$ is the inverse function of standard normal cumulative density function.

$$p_{f,SN}(t) = P[h_1(t) \le 0] \tag{6}$$
$$\beta_{SN}(t) = -\Phi^{-1}[p_{f,SN}(t)] \tag{7}$$

2.2 Probabilistic FM method

A fatigue model used for maintenance planning shall be able to give some predications on the time-variant fatigue damages, which can be compared to the results of operational inspections, and shall be able to incorporate effects of future inspections and maintenance. Thus, the FM method is adopted, in which fatigue deterioration process is explained by crack evolution with time. Based on probabilistic crack growth models, the effects of inspection results on the distribution of crack size and on failure probability can be taken into account by Bayesian techniques, and the maintenance effects are modelled in terms of mitigation of crack sizes [1, 34].

Paris' law [35] first relates crack growth rate to stress intensity factor. One dimensional crack growth mode given by Equation (8).

$$\frac{da}{dN} = C\Delta K^m, \qquad \Delta K_{th} \le \Delta K \le K_{mat} \tag{8}$$

where da/dN is crack growth rate, C and m are material parameters, K_{mat} is material fracture toughness, ΔK is stress intensity factor range and, ΔK_{th} is threshold value for ΔK.

Equation (9) is used to calculate the stress intensity factor range ΔK.

$$\Delta K = \Delta\sigma Y(a)\sqrt{\pi a} \tag{9}$$

where $Y(a)$ is geometry function and $\Delta\sigma$ is stress range.

The fatigue life at crack growth stage N_P can be obtained by integration of Equation (1) from an initial crack size a_0 to a critical crack size a_c, as per Equation (10). The crack size $a(t)$ at time t can be obtained by solving Equation (11) incrementally from the beginning time ($t = 0$) to a given time t when the accumulated fatigue loading is $N(t)$ cycles. The function $N(t)$ is often given, for example $N(t) = N_0 \cdot t$ (N_0 is annual number of fatigue cycles). An explicit formulation of the crack size $a(t)$ can be obtained based on Equation (11) and a geometry function $Y(a)$, which can be adopted from [36].

$$N_P = \frac{1}{\pi^{m/2} C \Delta\sigma^m} \int_{a_0}^{a_c} \frac{da}{a^{m/2} Y(a)^m} \tag{10}$$

$$da = \pi^{m/2} \cdot C \cdot \Delta\sigma^m \cdot a^{m/2} \cdot Y^m(a) \cdot dN(t) \tag{11}$$

A limit state function, $h_2(t)$, as per Equation (12), can be formulated based on crack size.

$$h_2(t) = a_c - a(t) \tag{12}$$

The FM approach is however highly sensitive to some input parameters, and statistical information on them are usually not sufficient. Figure 4 schematically shows the influence of uncertainty in initial crack size on crack growth prediction. Probabilistic methods are recognised to provide a sound theoretical basis for treating both inherent variability and modelling uncertainty [37].

Equations (13) and (14) give the failure probability ${p_f}^0(t)$ and reliability index $\beta^0(t)$ without consideration of operational maintenance.

$${p_f}^0(t) = P[h_2(t) \le 0] \tag{13}$$

$$\beta^0(t) = -\Phi^{-1}\left[{p_f}^0(t)\right] \tag{14}$$

2.2.1 Material properties

The fracture parameters C and m are generally obtained based on statistical analysis on specimen test data [38], and often treated as parameters that are unique to a type of material, although it is pointed out that their values are affected by the environment and the applied stress ratio [2]. The uncertainties in C and m are believed to be originated from the inhomogeneities in material, measurement method, procedure and statistical method for parameter estimation. In probabilistic analysis, C is typically treated as a variable and m is assumed to be constant [7].

2.2.2 Stress range and geometry function

Crack growth predictions are highly sensitive to the stress range $\Delta\sigma$ and geometry function $Y(a)$, which enter into the Equation (8) with the power of m [39]. The geometry function $Y(a)$ is affected by the initial crack size a_0 and fatigue exponent m. Some finite element methods are developed for modelling crack geometries and characterizing stress fields near the crack tips [40, 41]. However, finite element modelling is often time consuming. Geometry functions for common welded structural details can be found in [36].

2.2.3 Threshold of stress intensity factor

Crack growth threshold is generally thought to be a material property, though also depends on stress ratio [42]. In maintenance planning, the threshold value is typically assumed to be equal to zero [1, 15, 18]. This assumption is also adopted in this paper. It is believed that the assumption would not induce much inaccuracy, given that the effect of ΔK_{th} on crack growth prediction is small when a value less than $63\mathrm{N}\cdot\mathrm{mm}^{-3/2}$ is used [39]. Also, when constant-amplitude loading is applied, there is no sequence effect and the crack growth model neglecting the threshold can be used. This treatment is consistent with S-N method where sequence effects are also not considered [43].

2.2.4 Initial crack/flaw size

There are often initial flaws/cracks in structural components, especially in welded structures, caused by material defects (e.g. voids, brittle inclusions, corrosion pits, etc.) and machining & welding processes [44]. The initial crack sizes can be modelled with exponential [13, 34] or lognormal distributions [20, 45] or assumed to be constant [14].

2.2.5 Definition of failure and critical crack size

Cracks develop very quickly at the final fracture stage (Figure 4), so fatigue life is not very sensitive to a small change in critical crack size a_c. In engineering practice, a_c is often set to be equal to the component thickness T, as failure consequence is typically not obvious before through-thickness crack occurs [9, 15, 20, 43]. Failure criteria considering brittle fracture are seldom used in probabilistic inspection and maintenance planning due to computational costs. Also, materials in offshore structures are generally considered as ductile and brittle fracture is not supposed to be critical [46].

More sophisticated FM models are available to take into account more detailed aspects of fatigue and crack growth, e.g. Elber's Model [47], Bi-linear crack growth model [9], two-dimensional model [46]. Reviews on the probabilistic FM models are provided by [9, 11]. However, more sophisticated models normally require more input parameters, thus more difficult to gather enough data and thus more difficult to characterize model uncertainty [43]. In addition, computational costs increase significantly when a more sophisticated FM model is used. So, there is a need to achieve a trade-off between accuracy and practical implementation of a probabilistic optimization approach [43]. In fact, those sophisticated models are seldom applied to probabilistic maintenance optimization. The one-dimensional model (Equation (8)) has been adopted for reliability assessment of welded joints [39, 48], for inspection planning and updating [13-15] and for maintenance optimization [1, 18, 20, 49].

2.3 Calibration method for probabilistic FM model

It is often challenging to identify initial flaws/cracks and even harder to obtain a distribution of a_0 due to detection and measuring difficulties. A FM model is often calibrated to S-N curves, so that compatibility is achieved between FM and S-N approaches. Different calibration methods (in terms of calibration criterion and procedure) are available. Guidance on selecting calibration parameter and criterion can be found in [50]. Most often, such calibration is based on minimization of the difference between the reliability indexes by the FM and S-N method, e.g. using Equation (15) to obtain the mean value $E(a_0)$. In this paper, the initial crack size a_0 used in Section 6 follows [15, 46].

$$E(a_0) = \min_{a_0} \sum_{t=1}^{T_{SL}} [\beta^0(a_0, t\ ) - \beta_{SN}(t)]^2 \tag{15}$$

3 Maintenance strategy and repair effect

3.1 Maintenance strategy

A maintenance strategy defines the condition(s) to carry out a repair, e.g. following positive inspection results and exceedance of repair criteria. With a maintenance strategy defined, risk reductions by inspections & maintenance and associated costs can be assessed quantitatively at the decision-making time. Herein, a detection-based maintenance strategy, under which a repair is carried out upon crack detection by an inspection, is adopted in both holistic and separate decision-making. The risk-based HDM method developed is able to accommodate other maintenance strategies as well, via event tree analysis introduced in Section 5. Optimization methods for various of maintenance strategies addressed by [1, 18-21] are compatible with the HDM method developed herein.

3.2 Model for repair effect

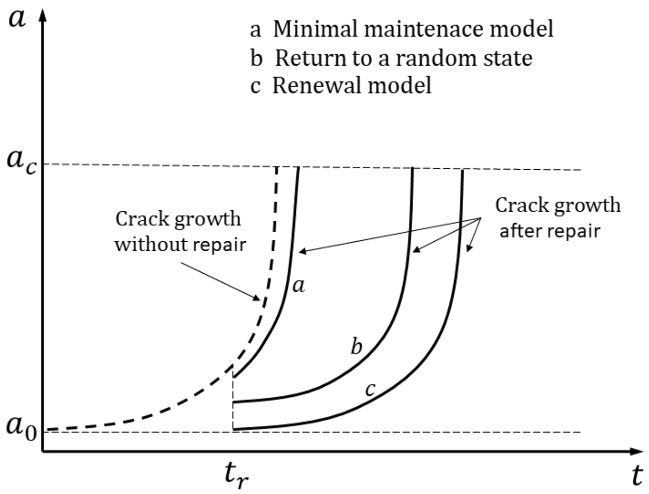

Figure 5: Illustration of models of repair effect

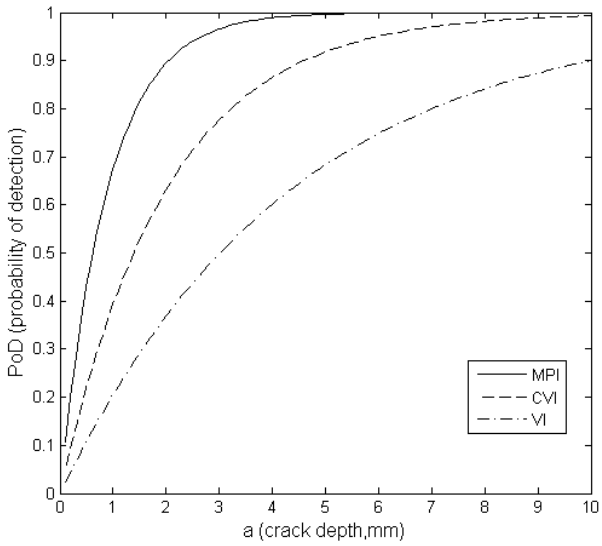

Figure 6: PoD curves for three inspection methods

At the operation stage, it is the repair (or replacement) activities that ultimately improves fatigue reliability and thus mitigates failure risks. Under a design stage point of view, planned inspections and maintenance can improve fatigue reliability only when a maintenance strategy is specified. Widely-used repair methods for cracks in structural engineering include [51, 52] drilling a stop hole, welding, welding plus post-weld treatment, replacement, grinding, etc. These methods can change a structural system physically, e.g. removing cracks, decreasing crack size, stopping or slowing down crack growth, etc., and thus change fatigue reliability. To assess effects of scheduled maintenance interventions on reliability and risk, it is necessary to quantify the effect of a repair.

Herein the same repair method and repair effect model is adopted throughout lifetime. It is assumed that after repair a structural component is renewed, i.e. the crack size after repair (at time t_r) is the same as the initial size a_0 as illustrated by curve 'c' in Figure 5. The repair effect model has been adopted by [49, 53-58]. Other repair effect models include those based on deterioration rate [59, 60]; the minimal maintenance model (i.e. 'as bad as old' model) such as curve 'a' in Figure 5 [61-63]; probabilistic repair effect models [64, 65], etc. But for high integrity structures, the probability of repair is very low, especially when a large repair crack size is adopted, and thus, the influence of repair effect model on fatigue reliability is marginal.

4 Probabilistic inspection modelling

There are uncertainties associated with any inspection method, and therefore, the reliability of an inspection method needs to be quantified before the effects of planned inspection and maintenance on risk mitigation can be formulated. Crack detection by an inspection is inherently probabilistic, because there are so many influential factors that are only partly controllable. Existing cracks can be detected sometimes but missed others. A positive indication can also be found to be false. In addition, crack detectability is also dependent on training, knowledge and performance of an inspector. Generally, the following factors can influence the probability of crack detection [51, 52]: crack characteristics (sizes, shape, location, etc.); reliability of instrumentation; environments where an inspection is carried out; inspection procedure; human factors associated with the inspector.

The detection reliability of an inspection method is often quantified via the probability of detection (PoD). The PoD is defined as the probability that a given crack of a fixed size can be detected by a given inspection method [51, 66]. Traditionally, PoD curves are obtained by inspection experiments. However, as there are so many factors affecting the PoD and need to be tested, experimental approaches usually are very expensive and time-consuming. Alternatively, simulation approaches can be used to obtain PoD curves [67-69].

$$PoD(a) = F(a) = 1 - \exp(-a/E(a_d)) \tag{16}$$

where $E(a_d)$ is the mean detectable crack size.

Herein the exponential PoD function given by Equation (16) is employed [12-14, 21, 34, 70-72]. By this function, uncertainty in crack detection is considered by modelling the detectable crack size, a_d, of an inspection method as an exponentially distributed variable. The PoD function is equal to the cumulative density function (CDF) of the variable a_d. Herein, three inspection methods are tested MPI, CVI, and CV, the mean detectable crack sizes are 0.89, 2 and 4.35 mm respectively [34, 49]. Figure 6 shows the PoD curves of these methods.

5 A risk-based holistic decision-making approach

5.1 Decision-making philosophy

Decision-making philosophy refers to how major decisions that affects lifetime fatigue performance (i.e. fatigue design, inspection and maintenance decisions) are made. Herein a holistically decision-making (HDM) method is proposed based on the same physical model for fatigue deterioration, i.e. the FM model (Section 2.2 and 2.3). By the HDM method, optimum values of decision variables in fatigue design, inspection and maintenance are derived holistically from an initial design perspective, and thus the optimum decisions are trackable and consistent with each other. A comparison method is the separate decision-method (SDM), by which the decision variables in fatigue design are optimized first adopting the FM model. Once fatigue design plans are established, decision variables in inspection & maintenance are optimized adopting the same FM model. The theoretical basis of the SDM and HDM methods is the same. The only difference lays on whether decisions are optimized separately or holistically.

5.2 Decision variables

The objective of this paper is to develop a risk-based decision-making method that can achieve the best compromise between design costs and maintenance costs considering failure consequences and uncertainties. Major decisions at the design and operation stages affecting the lifetime fatigue performance of a structural system are selected as decisions variables and are optimized under certain decision metrics.

5.2.1 Decision variables in fatigue design

Generally speaking, structural design against fatigue involves determination of materials, scantlings, joining methods and fabrication quality assurance procedure to ensure that the structure can survive identified loads with an acceptable failure probability. The traditional S-N design method adopts one safety factor, i.e. the so-called fatigue design factor (FDF), to counteract effects of all uncertainties. The FDF is one of the most important decision variables at the design stage. The FDF is typically determined based on engineering experience, expert options or qualitative assessment on the importance of the structural detail and, with little quantitative representation of operational inspections and maintenance in the design decision-making process.

Herein, the FDF is also selected as a major design variable at the design stage so that the developed method can be well comprehended by structural engineers. In the risk-based HDM method, the FDF and a major decision variable in maintenance planning are optimized simultaneously, in order to achieve the best compromise between the design costs corresponding to a FDF, and the maintenance costs corresponding to the maintenance decision variable. The FDF is correlated with the stress range $\Delta\sigma$ via the S-N curve of a structural detail, and the stress range $\Delta\sigma$ is assumed to be linearly correlated with the plate thickness T of a fatigue-prone structural detail (such as Figure 11). The actual decision variable is the plate thickness T, but all optimum values of plate thickness T are transformed to FDF. In summary, FDF is chosen as the main design variable, and it is affected by $\Delta\sigma$ and T.

Note that plate thickness T is an important parameter in structural design and in engineering practice it may not be determined only by design against fatigue limit state. The design envelope may include ultimate limit state, accidental limit state and other failure limit states or even fabrication and economic considerations. This paper however considers structural design of fatigue-critical components.

5.2.2 Decision variables in maintenance planning

Herein, maintenance planning means inspection and repair planning. Ideally, the following decisions can be made via optimum maintenance planning: areas of inspections, the number of inspections, the times and methods of inspections, repair criteria and methods, etc. Though it is possible to formulate an optimization problem with all those decision variables, it would be very difficult to solve the problem numerically as the areas and the number of inspections increase. To reduce the number of decision variables and possible solutions, some reasonable assumptions and practical operation constraints are introduced in developing optimum maintenance planning methods [1, 18, 20, 21, 55, 72]. These maintenance optimization methods can be incorporated into the risk-based HDM method developed to enhance its application to specific scenarios.

The number of inspections n and inspection times $t_1, t_2, \cdots, t_n$ are major decision variables in maintenance planning. The lifetime fatigue reliability β_L increases with an increase of n, as the probability increases that cracks are detected by more inspections and subsequently repaired. However, the expected costs of inspections C_I and repairs C_r also increase with n. Therefore, n is a decision variable that has significant influence on lifetime fatigue reliability β_L, failure risk C_F and lifetime total costs C_L. The inspection times $t_1, t_2, \cdots, t_n$ affect the probabilities of detection & repair p_r, and consequently have an impact on the expected repair costs C_r. Moreover, an inspection result of no detection provides additional information which can be utilized to update failure probability p_f and lifetime fatigue reliability β_L. Normally, there are different amount of changes in p_f and β_L, as a result of the additional information collected at different time $t_1, t_2, \cdots, t_n$ [16].

Herein, a periodic inspection policy following [55, 73-78] is adopted. The latter specifies that inspections are carried out at equal intervals, e.g. at Δt_{i}, $2\Delta t_{\mathrm{i}}$, $\cdots$, $n\Delta t_{\mathrm{i}}$. The inspection interval Δt_{i} (given in years) is a decision variable to be optimized. The periodic inspection policy is widely adopted in engineering practice due to convenience in maintenance implementation [55].

The areas of inspections are pre-selected, and the inspection methods are given. The same inspection method is applied to all maintenance interventions, and three methods are tested: MPI, CI, CVI. A detection-based maintenance strategy is adopted, and thus the repair criterion is actually determined by the selected inspection method. The methods of repairs are not considered as decision variables, since they are typically determined based on engineering practice and specific damage characteristics. The repair effect model adopted has been discussed in Section 3.2.

5.3 Metrics for optimal decision

The decision-making methods (HDM and SDM) are integrated with risk-based structural optimization, i.e. fatigue design and maintenance decisions are assessed by risk metric and optimized based on the metric. Main sources of uncertainty affecting the crack size and affecting the reliability of inspections are modelled explicitly and their impacts on holistic decision-making process are studied. Failure consequences are quantified, and risk quantification is performed in the design process. Structural scantling and maintenance activities are main risk mitigation measures against fatigue. Each set of values of decision variables represent a structural solution (more specifically, a structural dimension and maintenance plan). Each structural solution is associated with a specific level of lifetime failure probability and failure risk, and involves certain (design, construction, inspection, and repair) costs. These costs are structural investments on risk reduction. Integrated with holistic or separate decision-making method, risk-based structural optimization facilitates holistic or marginal trade-offs between structural investments and failure risks.

A comparison metric is lifetime fatigue reliability, which is a performance indicator taking into account sources of uncertainty affecting structural performance, but not failure consequences. A stronger structural solution, e.g. a thicker plate thickness and/or a shorter inspection interval, contributes to a higher lifetime fatigue reliability, but also leads to higher structural investments. Reliability-based structural optimization facilitates a cost-optimum structural solution that satisfies a given reliability requirement.

5.4 Limit state functions

The crack size $a(t)$ is probabilistic, due to uncertainties in the initial crack size a_0, stress range $\Delta\sigma$ and material property C. As $a(t)$ is probabilistic, the safety state of a structural system at time t (failure or survival) is also probabilistic. Structural failure is defined as occurrence of through-thickness crack, i.e. $a(t)$ exceeds a critical crack size a_c, which is equal to the plate thickness T. A fatigue limit state function is given by Equation (12), where $h_2 \leq 0$ signifies failure.

If an inspection is scheduled to time t, the inspection result (detection or no detection) is probabilistic as both the crack size $a(t)$ and the detectable crack size a_d of the adopted inspection method is probabilistic. If the inspection result is detection, a repair will be carried out. Thus, as the inspection result is probabilistic, the event of repair is also probabilistic. An event margin for inspection result is given by Equation (17).

$$D(t) = a_d - a(t) \tag{17}$$

Where $D(t) \leq 0$ when a crack is detected. Given that repair would be carried out upon detection, the event margin for repair is the same as the event margin for inspection.

5.5 Formulations of probabilities and reliabilities

Let the number of scheduled inspections be n, and the inspection times be $t_1, t_2, \cdots, t_n$. The probabilities of inspection and repair at the intervention times and lifetime failure probability need to be formulated before the fatigue reliability, failure risk and expected costs of design (and construction), inspection, repair and failure can be calculated. The probabilities of inspection, repair and failure are calculated based on event tree analysis [1, 18, 20].

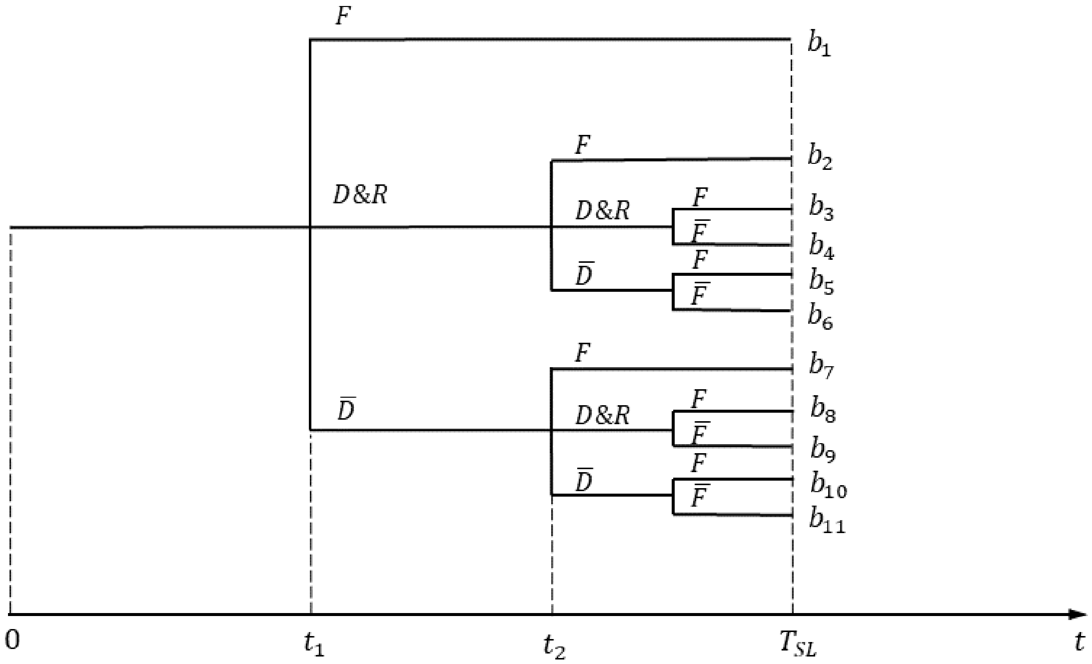

Figure 7: Event tree analysis under the detection-based maintenance strategy

Figure 7 illustrate event tree analysis where two inspections (n=2) are scheduled to t_1 and t_2. When the number of inspections n takes other values, event tree analysis can be done similarly. In Figure 7, F, D and R stand for failure, detection and repair respectively, $\bar{F}$ means survival and $\bar{D}$ denotes no detection. At a maintenance intervention time (e.g. at time t_1), there are three branches:

- B1: The structural component is failed.
- B2: The structural component is survived, and an inspection is carried out; a crack is detected and a repair is carried out.
- B3: The structural component is survived, and an inspection is carried out; a crack is not detected.

Based on Figure 7, the probability ($p_r{}^1(t_1)$) that a repair would be carried out at the 1st intervention at time t_1 is equal to the probability that the crack size a_{t_1} is not smaller than the detectable size a_d and smaller than the critical size a_c, given by Equation (18). As shown by Figure 7, the probability ($p_r{}^2(t_2)$) that a repair would be carried out at the 2nd intervention at time t_2 is comprised of two probabilities: the probability of repair at time t_2 conditional on that a repair has carried out at time t_1 (i.e. the event $D\&R$), and the probability of repair at time t_2 conditional on that a crack has not been detected at time t_1 (i.e. the event $\bar{D}$), as per Equation (19). When $n \geq 3$, the event tree is more complex than shown in Figure 7, but based on the same rationale, the probability ($p_r{}^n(t_n)$) that a repair would be carried out at the *n*th intervention at time t_n is given by Equation (20).

$$p_r{}^1(t_1) = P\left(a_d \leq a_{t_1} < a_c\right) \tag{18}$$

$$p_r{}^2(t_2) = p_r{}^1(t_1) \cdot p_r{}^1(t_2 - t_1) + P\left(a_{t_1} < a_d, a_d \le a_{t_2} < a_c\right) \tag{19}$$

$$p_r{}^n(t_n) = p_r{}^{n-1}(t_{n-1}) \cdot p_r{}^1(t_n - t_{n-1}) + P\left(a_{t_{n-1}} < a_d, a_d \le a_{t_n} < a_c\right) + \sum_{i=1}^{n-2} p_r{}^i(t_i) \cdot \ P\left(a_{t_{n-1}-t_i} < a_d, a_d \le a_{t_n - t_i} < a_c\right) \tag{20}$$

The probability of failure by time t is obtained by adding together the failure probabilities associated with all branches. When $t_1 < t \le t_2$, the probability of failure $p_f{}^1(t)$ is given by Equation (21). When $t_n < t \le T_{SL}$ ($n \ge 2$, T_{SL} is required service life), the probability of failure $p_f{}^n(t)$ is given by Equation (22). Lifetime failure probability is the failure probability when $t = T_{SL}$.

When $t_1 < t \le t_2$,

$$p_f{}^1(t) = p_f{}^0(t_1) + p_r{}^1(t_1) \cdot p_f{}^0(t - t_1) + P\left(a_{t_1} < a_d, a_t \ge a_c\right) \tag{21}$$

When $t_n < t \le T_{SL}$ ($n \ge 2$),

$$p_f{}^n(t) = p_f{}^{n-1}(t_n) + p_r{}^n(t_n) \cdot p_f{}^0(t - t_n) + P\left(a_{t_n} < a_d, a_t \ge a_c\right) + \sum_{i=1}^{n-1} p_r{}^i(t_i) \cdot P\left(a_{t_n - t_i} < a_d, a_{t-t_i} \ge a_c\right) \tag{22}$$

The probabilities of conducting inspection ($p_i{}^1(t_1), p_i{}^2(t_1), \cdots, p_i{}^n(t_1)$) at the intervention time $t_1, t_2, \cdots, t_n$ are conditional on the structural system is survived at the intervention times, given by Equation (23-(25)

$$p_i{}^1(t_1) = 1 - p_f{}^0(t_1) \tag{23}$$
$$p_i{}^2(t_1) = 1 - p_f{}^1(t_2) \tag{24}$$
$$p_i{}^n(t_1) = 1 - p_f{}^{n-1}(t_n) \tag{25}$$

Reliability index $\beta^i(t)$ (i=0, 1, 2, ⋯, n) corresponding to a failure probability $p_f{}^i(t)$ is given by Equation (26). Lifetime fatigue reliability index β_L considering n planned maintenance interventions is given by Equation (27).

$$\beta^i(t) = -\Phi^{-1}\left[p_f{}^i(t)\right] \quad (i=0, 1, 2, \cdots, \ n) \tag{26}$$
$$\beta_L = -\Phi^{-1}\left[p_f{}^n(T_{SL})\right] \tag{27}$$

5.6 Quantitative risk analysis

Failure risk C_F is defined as the product of failure probability p_f and failure consequences c_{f0}, as per Equation (28). The risk is understood as potential loss associated with a structural (design and maintenance) solution.

$$C_F = p_f \cdot c_{f0} \tag{28}$$

Failure consequences c_{f0} are quantified via the approach as follows. An existing fatigue design plan T_0 was previously obtained by traditional S-N design method, without quantitatively taking into account effects and costs of operational inspections & maintenance. It has been proved by engineering practice that the design plan T_0 is associated with the minimum life cycle total costs (C_{L0}) defined by Equation (29). In Equation (29), the design (and construction) costs (C_D) associated with the design plan T_0 are given in Section 5.7, and the failure risk (C_{F0}) is defined by Equation (30), in which the failure probability (p_{f0}) is calculated by the probabilistic S-N method introduced in Section 2.1. Then the value of failure consequences c_{f0} which makes the C_{L0} in Equation (29) minimal can be derived.

$$C_{L0} = C_D + C_{F0} \tag{29}$$
$$C_{F0} = p_{f0} \cdot c_{f0} \tag{30}$$

5.7 Life cycle cost analysis

By the risk-based holistic decision-making (HDM) approach, the life cycle total costs C_L are comprised of design (and construction) costs C_D, inspection costs C_I, repair costs C_R, and failure risks (potential economic losses) C_F, as formulated by Equation (31). Herein the sum of inspection costs C_I and repair costs C_R are called maintenance costs C_M (Equation (32)). Total structural investments C_{INT}, given by Equation (33), is defined as the sum of design (and construction) costs C_D and maintenance costs C_M. Note that in this paper, life cycle costs are evaluated against the same time length, i.e. required service life of the structure T_{SL}.

$$C_L = C_D + C_I + C_R + C_F \tag{31}$$
$$C_M = C_I + C_R \tag{32}$$
$$C_{INT} = C_D + C_M \tag{33}$$

By a separate decision-making (SDM) method, optimization of fatigue design plan and maintenance plan is carried out separately and sequentially. More specifically, operational maintenance (and associated costs) is not include in the design optimization formulation, and structural design plan (and associated costs) is fixed and not included in the maintenance optimization formulation. The life cycle costs formulated at the design optimization (C_{L1}) and maintenance optimization (C_{L2}) stages are given by Equations (34) and (35) respectively. The failure risks at the design optimization (C_{F1}) and maintenance optimization stage (C_{F2}) are calculated by Equations (36) and (37) respectively, in which ${p_f}^0(T_{SL})$ and ${p_f}^n(T_{SL})$ are lifetime failure probabilities neglecting and considering maintenance interventions and calculated by Equations (13) and (22) respectively.

$$C_{L1} = C_D + C_{F1} \tag{34}$$
$$C_{L2} = C_I + C_R + C_{F2} \tag{35}$$
$$C_{F1} = {p_f}^0(T_{SL}) \cdot c_{f0} \tag{36}$$
$$C_{F2} = {p_f}^n(T_{SL}) \cdot c_{f0} \tag{37}$$

Herein an Equation (38) is proposed for the design (and construction) costs C_D associated with a design plan. The equation relates C_D to design plate thickness T and also to the failure risk C_{F0} associated with a design plan. It is believed that the equation implicitly takes all determinants of C_D into account, by correlating C_D with C_{F0}. Apart from plate thickness T (the main design variable), C_D is affected by other parameters that determined at the design stage, e.g. spacings of stiffeners, local geometry, materials, fabrication techniques, etc. These parameters have not been explicitly included in the optimization formulation as design variables, but their influences on C_D are represented via C_{F0}. The failure risk C_{F0} is a composite performance indicator that can show the influences of all design parameters. Favourable choices of design parameters (e.g. good local geometry with low level of stress concentration, material with high fatigue performance and fabrication techniques with low residual stress) would contribute to a lower failure probability and risk, and thus the calculated design (and construction) costs by Equation (38) are high, and vice versa.

$$C_D = \frac{T^2}{\sqrt[3]{C_{F0}}} \tag{38}$$

The expected inspection costs C_I and repair costs C_R are given by Equations (39) and (40) respectively. The equations are formulated by adding together the expected costs of inspection and repair associated with each maintenance intervention [21, 72, 79]. Alternatively, the maintenance costs (C_M) can be obtained via Equation (41), where the expected inspection and repair costs of are formulated by adding together the expected inspection and repair costs associated with each branch in the event tree analysis, as illustrated by Figure 7 [1].

$$C_I = \sum_{k=1}^{n} p_i^k \cdot c_{i0}^k \cdot \frac{1}{(1+\gamma)^{t_k}} \quad (39)$$

$$C_R = \sum_{k=1}^{n} p_r^k \cdot c_{r0}^k \cdot \frac{1}{(1+\gamma)^{t_k}} \quad (40)$$

$$C_M = \sum_{k=1}^{N_b} p(b_k) \cdot C_k \quad (41)$$

where n is the number of scheduled maintenance interventions in the service life; c_{i0}^k and c_{r0}^k are costs for the k^{th} inspection and repair respectively; p_i^k and p_r^k are the probability of the k^{th} inspection and repair are carried out; t_k is the times of the k^{th} inspection; γ is average annual discount rate of money; $p(b_k)$is the probability of occurrence of branch k; C_k is the expected total inspection and repair costs associated with branch k and N_b is the number of branches. For example, in Figure 7, there are 11 branches in total, and thus N_b=11, The branches are numbered 1, 2, …, 11 respectively. Let k=1, calculate the probability of occurrence of the branch 1 (i.e. $p(b_1)$) and expected total inspection & repair costs associated with branch 1 (C_1). Then Let k=2, calculate the probability of occurrence of the branch 2 (i.e. $p(b_2)$)and expected total inspection & repair costs associated with branch 2 (C_2). Similarly, lastly, Let k=11, calculate the probability of occurrence of the branch 2 (i.e. $p(b_{11})$)and expected total inspection & repair costs associated with branch 2 (C_{11}). Then total maintenance costs can be obtained by Equation (41).

When the same inspection method and repair method is applied to all maintenance interventions in the service life, then $c_{i0}^k = c_{i0}$, $c_{r0}^k = c_{r0}$. This paper aims at studying how the best balance between design costs C_D and maintenance costs C_M can be achieved by the risk-based holistic decision-making method. Therefore, the sum of C_I and C_R are evaluated, as opposed to C_I or C_R individually. A fix relationship between c_{i0} and c_{r0}, given by Equation (42), is adopted to reduce the number of input parameters. The ratio c_{r0}/c_{f0} is an input parameter that will be varied to investigate the influence of failure consequences.

$$c_{i0} = 0.1c_{r0} \quad (42)$$

5.8 Optimization problem formulation

Figure 8 gives a flowchart for the proposed risk-based HDM method. The main idea is that by a risk-based HDM method, structural systems are managed holistically based on the same fatigue deterioration model, considering major engineering decisions (i.e. fatigue design, inspection and maintenance) and uncertainties affecting structural fatigue performance. The optimization problem is formulated by Equation (43). The FDF is defined as the ratio of required fatigue resistance (in years) to required service life (in years). Required fatigue resistance should not be shorter than required service life, and thus the FDF should not be smaller than 1. Herein, periodic inspections are considered. The inspection time interval Δt_i (given in years) isn't longer than 15 years so that at least one inspection would be carried out in the entire service life, and it isn't shorter than 2 years so that the number of inspections are not larger than 15.

find: $FDF, \Delta t_i$
which minimize: C_L (43)
subject to: $FDF \geq 1$, $2 \leq \Delta t_i \leq 15$

The following points summarize the proposed risk-based HDM method:

- The decision variables in fatigue design, inspection & maintenance jointly determine the lifetime fatigue reliability β_L (Equation (27)) and expected life cycle total costs C_L (Equation (31)).
- Conversely, the decision variables as well as lifetime reliability level β_L are optimized simultaneously based

on minimization of C_L.

- The lifetime fatigue reliability β_L associated with a structural scantling is calculated based on a probabilistic FM model, and the β_L is updated by a maintenance plan based on the same FM model.
- Inspection result is unknown at the decision-making time, but the distribution of possible results, i.e. the probabilities of detection and no detection, can be obtained based on probabilistic modelling of crack growth and inspection reliability.
- The repair decision is upon inspection result following a detection-based maintenance strategy.
- An inspection result of detection would lead to a repair being carried out and thus a lower lifetime failure probability p_f (and a higher β_L), while an inspection result of no detection provides an evidence, from which a lower failure probability p_f can be inferred based on Bayes' theorem.
- In case of a repair being carried out, the failure probability after repair is obtained based on the adopted repair effect model and probabilistic FM model.
- The design (and construction) costs C_D are related to a structural scantling and design failure probability (Equation (38)); the expected maintenance costs C_M are related to a maintenance plan and distributions of crack size at the maintenance intervention times (Equation (41)); the failure risk C_F is related to a structural scantling, a maintenance plan and the uncertainties associated with the FM model (Equation (28)).

The risk-based HDM method is compared to two alternative methods: the reliability-based HDM method (Figure 9, Equation (44)) and the risk-based SDM method (Figure 10, Equations (45) and (46)).

find: $FDF, \Delta t_i$
which minimize: C_{INT} (44)
subject to: $FDF \geq 1$, $2 \leq \Delta t_i \leq 15$, $\beta_L \geq \beta_t$

Step 1:
find: FDF
which minimize: C_{L1} (45)
subject to: $FDF \geq 1$
Step 2:
find: Δt_i
which minimize: C_{L2} (46)
subject to: $2 \leq \Delta t_i \leq 15$

The proposed and comparison methods differ from each other in the decision-making philosophy (holistic or separate) and metric for optimum decision (risk or reliability). The three methods are explained briefly as follows.

- Risk-based HDM method: structural scantling (plate thickness) and maintenance plan (inspection interval) are optimized simultaneously based on minimization of life cycle costs (i.e. Equation (43)).
- Reliability-based HDM method: structural scantling and maintenance plan are optimized simultaneously based on minimization of structural investments (i.e. Equation (44)) with a constraint on reliability.
- Risk-based SDM method: First, structural scantling is optimized based on minimization of the sum of design costs and failure risks (i.e. Equation (45)). Second, maintenance plan is optimized based on minimization of the sum of maintenance costs and failure risks (i.e. Equation (46)).

Noted that herein the examined optimization problems, formulated by Equations (43) – (46), are all single objective optimization problems. In Equations (43), (45) and (46), the risk metric C_F, C_{F1} and C_{F2} are integrated into the life cycle costs C_L, C_{L1} and C_{L2} respectively by Equations (31), (34) and (35); while in Equation (44), the reliability metric β_L is represented as a constraint.

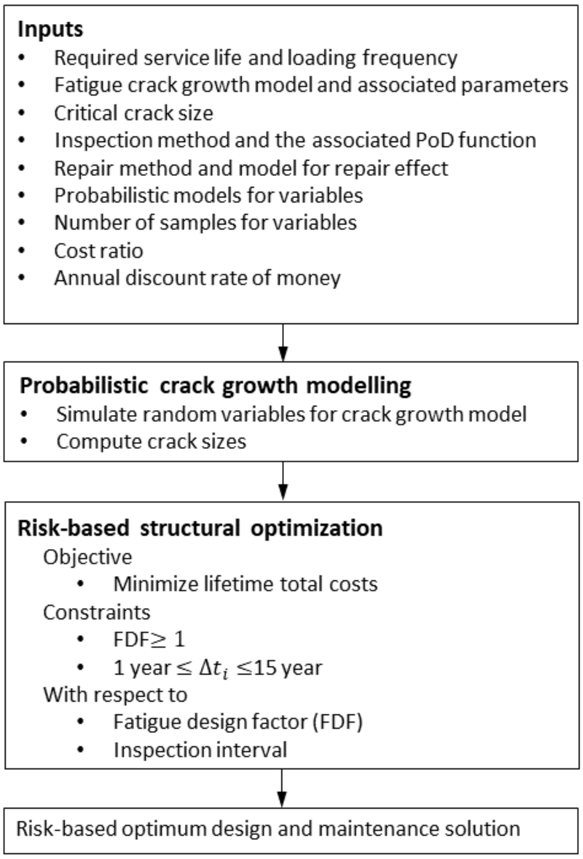

Figure 8: Flowchart for the risk-based HDM approach

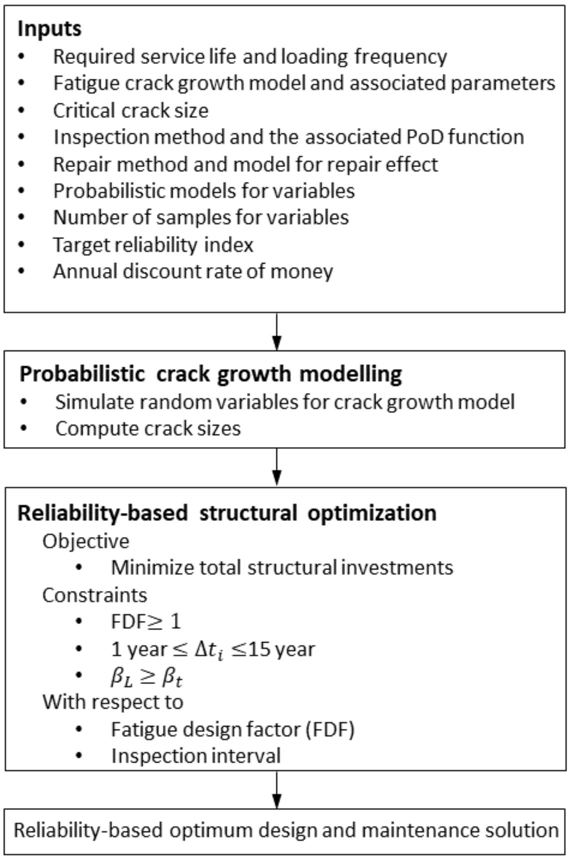

Figure 9: Flowchart for the reliability-based HDM approach

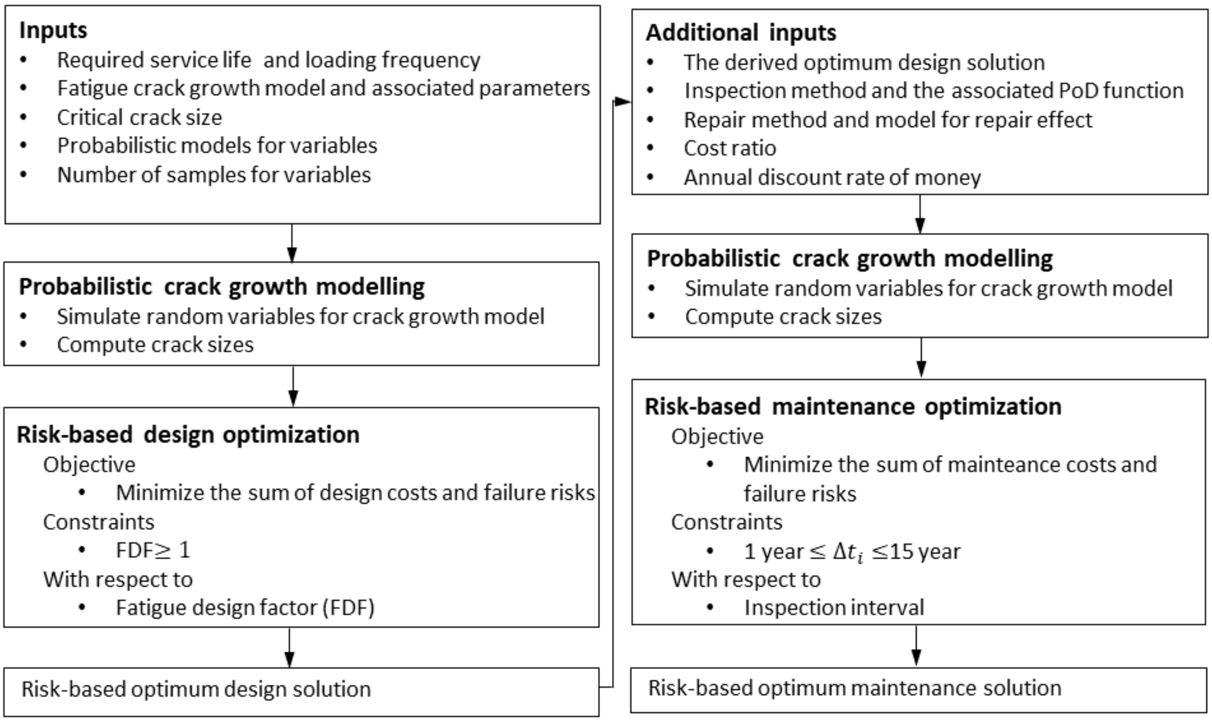

Figure 10: Flowchart for the risk-based separate decision-making (SDM) method

6 A numerical example

The proposed risk-based HDM method and comparison methods are demonstrated on a stiffened plate (Figure 11) typically found in ship structures. Welded T joints are very common in ship structures that are susceptible to fatigue failures due to cyclic wave loading. Failures of welded T joints are also common in other steel structures subjected to cyclic loading, e.g. offshore installations, offshore wind turbine foundations, bridge decks, etc. Welded joints often represent the weakest areas in structural integrity, as cracks are likely to initiate along the welding toes due to the presence of welding defects. Crack growth can lead to fracture of the structural detail and cause subsequent failures of adjacent structural components. Fatigue performance and reliability of welded joints should be assessed at the design stage and maintained at the operation stage. The proposed method and comparison methods are used to derive an optimum structural solution (structural scantling and maintenance plan) for the structural detail.

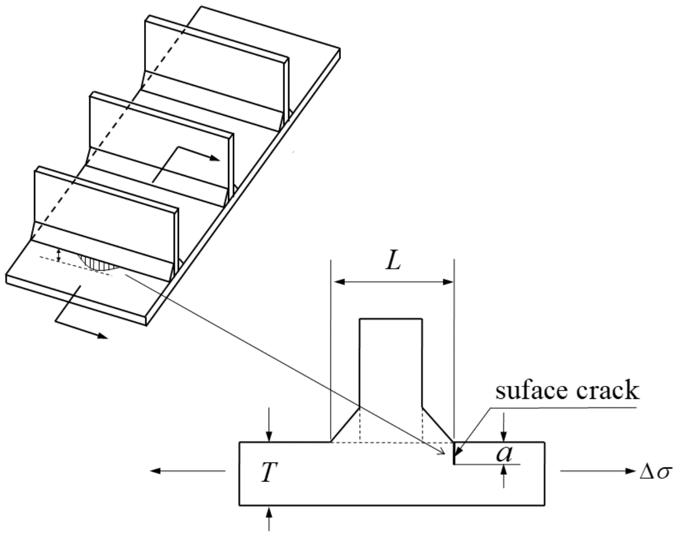

Figure 11: The studied fatigue-prone structural detail

6.1 Probabilistic models

The required service life of the ship is T_{SL}=30 years. As a long T_{SL} is required, multiple maintenance interventions may be needed. The fatigue loading is wave loading with a frequency of about 0.16 Hz, which corresponds to $N_0 = 5 \times 10^6$ cycles per year [15, 46]. The fatigue resistance of the structural detail is categorized as F class and given by a two-segment S-N curve given by Equation (1). The coefficients associated with F class S-N curve is given by ship design rules [7]. Based on engineering practice, the reference optimum structural design is $T_0 = 25\ \mathrm{mm}$, fatigue design factor FDF=3, and the allowed equivalent stress range is $\Delta\sigma_0 = 19.39\ \mathrm{MPa}$. Table 1 summarizes the input parameters.

Table 1: Design Parameters for the structural detail

Parameter	Unit	Value
T_{SL}	Year	30
N_0	Cycle	5×10^6
$\log_{10} \overline{a_1}$	[N, mm]	11.855
$\log_{10} \overline{a_2}$	[N, mm]	15.091
m_1	-	3
m_2	-	5
T_0	mm	25
$\Delta\sigma_0$	MPa	19.39

Parameter uncertainties associated with the initial crack size a_0, the crack growth rate C and modelling uncertainty in the stress range $\Delta\sigma$ in the FM model are considered. It is generally acknowledged that these uncertainties are influential on the crack growth modelling results obtained with the FM model [48]. The initial crack size a_0 is assumed to follow an exponential distribution, and the calibrated mean value $E(a_0) = 0.04$ [15, 46]. The uncertainty in $\Delta\sigma$ originate from load description, the methods used for calculation of structural response, stress concentration factor and the effect of welding notch, etc. In this paper, the uncertainty in $\Delta\sigma$ are represented by a multiplier B, which follows a normal distribution with mean value $E(B) = 1$ and standard deviation (SD) $\mu(B) = 0.15$ [70]. The crack growth rate C is usually thought to be a material property. In marine engineering, C is often considered as a lognormally distributed variable and m is a constant equal to 3 [15, 46]. It is widely adopted that the fatigue damage at failure Δ in the S-N model follows a lognormal distribution with mean value $E(\Delta) = 1$ and the standard deviation (SD) $\mu(\Delta) = 0.30$ [14, 18, 26]. The detectable crack size a_d of an inspection method (Section 3), is modelled as an exponentially distributed variable [34, 49]. The statistical descriptors for all variables are listed in Table 2.

Table 2: Variables and their characteristic values used in probabilistic analysis

Variable	Distribution	Unit	Mean	SD
a_0	Exponential	mm	0.04	0.04
$\log_{10} C$	Normal	[N, mm]	-12.74	0.11/0.14
B	Normal	-	1.00	0.15
a_d	Exponential	mm	0.89/2.00/4.35	0.89/2.00/4.35
Δ	lognormal	-	1	0.30

According to the uncertainty categorization defined in [80-82], uncertainties in the initial crack size a_0 and material fracture property C are aleatory uncertainty, which are mainly due to inherent variabilities in material qualities and properties. Uncertainties in the stress range $\Delta\sigma$ (represented by a multiplier B) are epistemic uncertainty, which are mainly due to uncertainties in load and stress analysis methods, such as uncertainties in finite element analysis. Uncertainties in the fatigue damage at failure Δ include both aleatory and epistemic uncertainty, i.e. variability inherent in the material and modelling uncertainty in Miner's rule. Uncertainties in the detectable crack size a_d of an inspection method include both aleatory and epistemic uncertainty, because a_d is affected by both inherent variabilities in crack characteristics and uncertainties in a non-destructive evaluation method, which can be viewed as a sub-model.

6.2 Methods

Monte Carlo simulations are carried out to calculate the probabilities and reliability indexes, with 5×10^6 samples for each variable. It is checked that a larger number of samples do not lead to much change in the results. Lifetime fatigue reliability without maintenance is 0.78, which is low due to a long, required service life. So, maintenance interventions are scheduled to increase operational reliability, which normally increases with more maintenance interventions. The proposed risk-based HDM method and two comparison methods formulated in Section 5 are applied to the structural detail to seek for optimum structural scantling and maintenance plan. Major decision variables are plate thickness T (transformed to corresponding FDF), and inspection interval Δt_i. Sensitivities of obtained optimal solution $(FDF, \Delta t_i)_{opt}$, fatigue reliability β_L, life cycle costs C_L and structural investment C_{INT} to cost ratio c_{r0}/c_{f0}, to adopted inspection method and to level of uncertainty are examined.

Five values of cost ratio c_{r0}/c_{f0} are tested (0.1, 0.01, 0.001, 0.0001 and 0.00001) to show sensitivity of derived optimum structural solution $(FDF, \Delta t_i)_{opt}$ to failure consequences. The unit of the obtained costs are the costs of an inspection. When reliability-based optimization is applied, three levels of target reliability index β_t (2.5, 3.0, and 3.5) are imposed respectively as an optimization constraint to study the influence of given target reliability on the optimum solutions derived by reliability-based optimization. Other optimization constraints are: $FDF \geq 1$ and $2 \leq \Delta t_i \leq 15$. Herein integer values of FDF and Δt_i are considered, because in design codes and standards of marine & offshore structures, FDF and Δt_i normally take integer values. As the number of feasible solutions is not large, an exhaustive search algorithm is adopted to derive the optimum values. It is checked that in this optimization problem local minima are not present, which if present, can be addressed by the technique developed in [83].

Sensitivities of derived optimum structural solution $(FDF, \Delta t_i)_{opt}$ to adopted inspection method and level of uncertainty are also investigated. Firstly, MPI and the probabilistic models in Table 1 are adopted for optimum structural fatigue design and maintenance planning. Then CVI and VI are adopted respectively. It is considered that the costs of the inspection methods satisfy MPI>CVI>VI. It is adopted that $c_{i0,\mathrm{CVI}}=0.35 \cdot c_{i0,\mathrm{MPI}}$ and $c_{i0,\mathrm{VI}}=0.2 \cdot c_{i0,\mathrm{MPI}}$, based on some references [34, 49]. Lastly, the standard deviation in $\log_{10} C$ is increased to 0.14 to show the influence of level of uncertainty on derived optimum structural solution $(FDF, \Delta t_i)_{opt}$ derived by the risk-based HDM method.

6.3 Results and discussions

6.3.1 Comparisons of the HDM and SDM approaches

6.3.1.1 Life cycle costs and sensitivity to cost ratio

Table 3: Optimum results by the risk-based HDM approach

	c_{r0}/c_{f0}	0.1	0.01	0.001	0.0001	0.00001
Risk-based design and maintenance holistic optimization	$(FDF, \Delta t_i)_{opt}$	(8,15)	(6,15)	(3,6)	(2,3)	(1,2)
	T (mm)	30.4	28.7	25.0	23.1	20.1
	n	1	1	4	9	14
	C_L	20193	3540	823.5	163.8	48.4
	C_{INT}	20063	3035	775.8	159.5	30.6
	β_L	3.415	3.025	3.679	4.252	3.923
	C_D	2797	1010	125.0	46.6	12.7
	C_M	17266	2025	650.8	112.9	17.9
	C_F	129.8	505.3	47.7	4.3	17.8

Table 4: Optimum results by the risk-based SDM approach

Risk-based design optimization	FDF_{opt}	9				
	T (mm)	31.1				
	C_D	4356				
	C_{F0}	4010				
	C_{L0}	8366				
	β_{L0}	2.332				
	c_{r0}/c_{f0}	0.1	0.01	0.001	0.0001	0.00001
Risk-based Maintenance optimization	$\Delta t_{i,opt}$ (year)	15	15	15	10	8
	n	1	1	1	2	3
	C_L	20665	6047	4585	4387	4360
	β_L	3.594	3.594	3.594	4.266	4.774
	C_M	16243	1624	162.7	26.6	3.6
	C_F	66.3	66.3	66.3	4.0	0.4

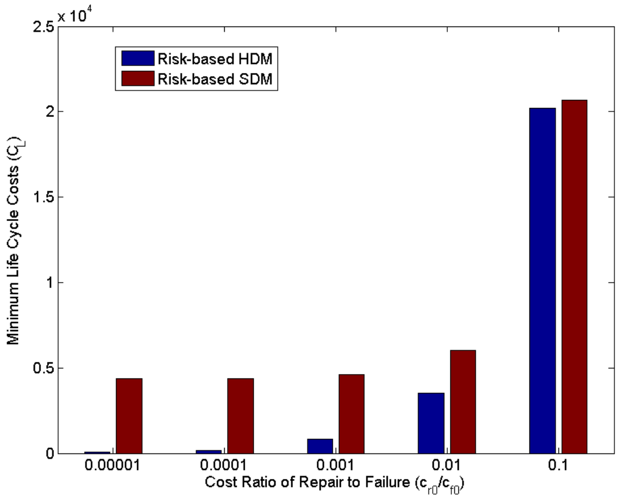

Figure 12: Minimum life cycle costs by the proposed and risk-based SDM approaches

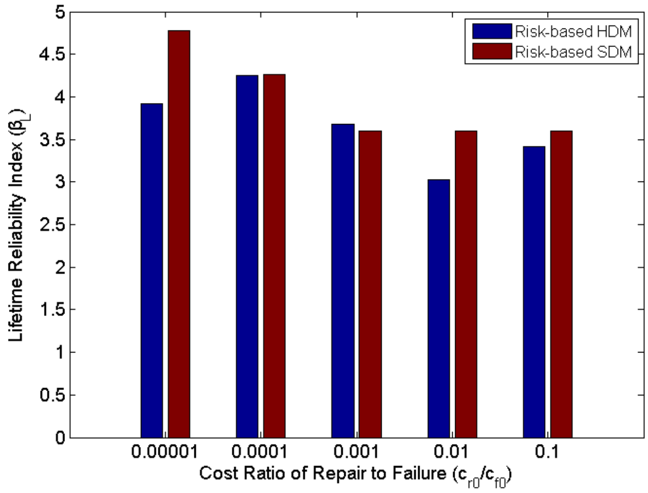

Figure 13: Lifetime reliability index by the proposed and risk-based SDM approaches

Tables 3 and 4 and Figure 12 show that for all c_{r0}/c_{f0} ∈[0.00001, 0.1], the proposed HDM method can result optimum structural (design and maintenance) plans associated with less life cycle costs C_L than the SDM method. The advantage of the HDM approach in cost reduction is more obvious with a lower cost ratio c_{r0}/c_{f0}. For c_{r0}/c_{f0}=0.00001, the min C_L by the HDM approach is 48.4, while the min C_L by the SDM approach is 4360, which is almost 90 times higher. The finding indicates that the proposed risk-based HDM approach is well suitable for those scenarios where the repair costs for a fatigue-critical detail are low compared with its failure consequences.

Table 3 shows that the proposed approach results in a weaker structural scantling (i.e. a smaller FDF) and a stronger maintenance plan (i.e. a shorter inspection interval Δt_i) with a lower c_{r0}/c_{f0}. This feature means that the HDM approach can result in optimum structural (design and maintenance) plans adaptively to the cost ratio, which has not been adequately captured by the SDM approach.

It can be seen from Tables 3 and 4 that a majority of the cost reductions by the HDM approach originate from lower design costs (C_D). In other words, a weaker design plan (i.e. a smaller FDF) can often be justified by explicitly quantifying and considering the benefits of operational maintenance to risk mitigation at the initial design stage.

6.3.1.2 lifetime fatigue reliability and sensitivity to cost ratio

While the min C_L is lower, the fatigue reliability index β_L obtained by the HDM approach is above 3 under all cost ratios (Table 3), which is high enough to meet the reliability requirement for common structural details. For example, the target reliability index β_t is 3.0 for structural details with very serious failure consequences in tanker ships [14, 84]. When cost ratio $c_{r0}/c_{f0} = \mathbf{0.01}$, the min C_L by the HDM (823.5) is significantly lower than the SDM approach (4585), and the optimum β_L (3.679) is slightly higher than by the SDM approach (3.594). For other cost ratios, the optimum β_L derived by the HDM approach is slightly lower than by the SDM approach.

In summary, the risk-based HDM approach can result in structural (design and maintenance) plans associated with lower life cycle costs that represent a null or only a small compromise in fatigue reliability. Compared to the SDM approach, the HDM approach allows for the cost ratio c_{r0}/c_{f0} and the effectiveness of two risk mitigation measures (structural scantling and operational maintenance), achieving optimum utilization of the two measures and thus optimum allocation of resources to the structural design and operation stage.

6.3.2 Comparisons of risk-based and reliability-based HDM approaches

6.3.2.1 Lifetime fatigue reliability

Table 5 (a): Optimum results by the reliability-based HDM approach (β_t=2.5)

	c_{r0}/c_{f0}	0.1	0.01	0.001	0.0001	0.00001
Reliability-based design and maintenance holistic optimization	$(FDF,\Delta t_i)_{opt}$	(8,15)	(5,15)	(3,10)	(2,8)	(1,4)
	T (mm)	30.4	27.7	25.0	23.1	20.1
	n	1	1	2	3	7
	C_L	20221	3887	1684	1793	1084
	C_{INT}	20063	2784	573.5	116.1	26.5
	β_L	3.415	2.758	2.775	2.637	2.777
	C_D	2797	554.7	125.0	46.6	12.7
	C_M	17266	2230	448.5	69.5	13.8

Table 5 (b): Optimum results by the reliability-based HDM approach (β_t=3.0)

	c_{r0}/c_{f0}	0.1	0.01	0.001	0.0001	0.00001
Reliability-based design and maintenance holistic optimization	$(FDF,\Delta t_i)_{opt}$	(8,15)	(6,15)	(4,10)	(2,6)	(1,3)
	T (mm)	30.4	28.7	26.5	23.1	20.1
	n	1	1	2	4	9
	C_L	20221	3515	967.5	557.4	252.6
	C_{INT}	20063	3035	674.3	123.8	27.5
	β_L	3.415	3.025	3.203	3.077	3.269
	C_D	2797	1010	279.6	46.6	12.7
	C_M	17266	2025	394.6	77.2	14.8

Table 5 (c): Optimum results by the reliability-based HDM approach (β_t=3.5)

	c_{r0}/c_{f0}	0.1	0.01	0.001	0.0001	0.00001
Reliability-based design and maintenance holistic optimization	$(FDF,\Delta t_i)_{opt}$	(9,15)	(5,10)	(3,6)	(2,4)	(1,2)
	T (mm)	31.1	27.7	25.0	23.1	20.1
	n	1	2	4	7	14
	C_L	20658	4295	834.9	182.9	42.3
	C_{INT}	20591	4107	775.8	151.5	30.6
	β_L	3.590	3.532	3.679	3.788	3.923
	C_D	4356	554.7	125.0	46.6	12.7
	C_M	16235	3552.5	650.8	105.0	17.9

The optimization formulation (Equation (43)) shows that the structural plans (i.e. structural scantling T and maintenance plan Δt_i) derived by the risk-based HDM approach are optimum in terms of the min expected C_L, i.e. the best trade of between structural investments C_{INT} and failure risks C_F. The derived β_L is optimum in terms of the min expected C_L, under given uncertainties and cost ratio. The risk-based HDM approach thus facilitates optimization of both β_L and structural plans. Table 3 and Figure 13 show that the β_L derived by the risk-based HDM approach is generally larger with a smaller cost ratio c_{r0}/c_{f0}, which indicates that the resulting β_L is higher when the failure consequences are larger. Therefore, the risk-based HDM approach can result in optimum structural plans associated with the min life cycle costs C_L and an optimum β_L which is in proportion to the failure consequences.

Equation (44) shows that there is a constraint on the fatigue reliability in the reliability-based HDM approach, i.e. $\beta_L \geq \beta_t$, which means that the derived optimum structural plans can achieve a min β_L defined by the constraint β_t. However, the achieved β_L may not be optimum in terms of life cycle costs C_L. Tables 5 (a), (b) and (c) show that the fatigue reliability indexes β_L obtained by the reliability-based HDM approach do not change in proportion to the cost ratio c_{r0}/c_{f0}.

6.3.2.2 Life cycle costs

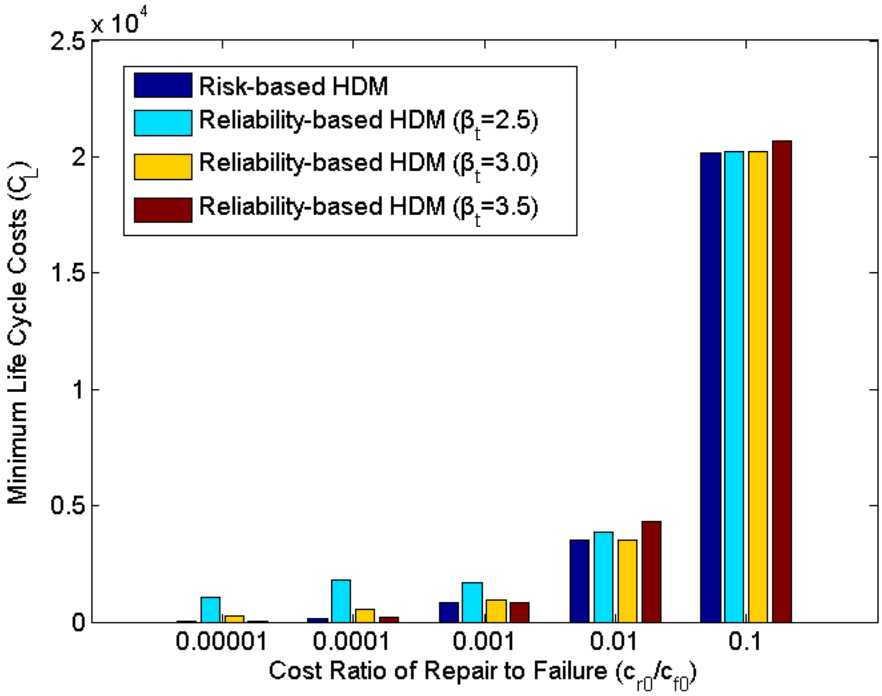

Figure 14: Minimum life cycle costs by the proposed and reliability-based HDM approaches

Table 3, Tables 5 (a), (b) and (c) and Figure 14 show that under all cost ratios examined, the min C_L derived by the risk-based HDM approach are lower than the reliability-based HDM approach. These results are the same as expected, because the optimization objective of the risk-based approach is to minimize C_L, while the optimization objective of the reliability-based approach is to minimize C_{INT}, under a given constraint on target reliability level β_t.

6.3.2.3 Structural investments

Table 6: Comparisons of the risk-based and reliability-based HDM approaches

		Risk-based HDM	Reliability-based HDM
Lifetime fatigue reliability β_L	$\beta_t > \beta_{l,opt}$	Lower	Higher
	$\beta_t < \beta_{l,opt}$	Higher	Lower
	$\beta_t \cong \beta_{l,opt}$	The same	The same
Life cycle costs C_L	$\beta_t > \beta_{l,opt}$	Lower	Higher
	$\beta_t < \beta_{l,opt}$	Lower	Higher
	$\beta_t \cong \beta_{l,opt}$	The same	The same
Structural investments C_{INT}	$\beta_t > \beta_{l,opt}$	Lower	Higher
	$\beta_t < \beta_{l,opt}$	Higher	Lower
	$\beta_t \cong \beta_{l,opt}$	The same	The same

Although the optimization objective of the reliability-based approach is to minimize structural investments C_{INT} under a reliability constraint, the derived C_{INT} may not be minimum globally. Given a specific β_t and c_{r0}/c_{f0}, the structural investments C_{INT} by the risk-based HDM approach can be equal to, lower or higher than the reliability-based approach. Three cases are distinguished and discussed below, where β_t is the prescribed reliability target in the reliability-based approach, and $\beta_{l,opt}$ is the optimum reliability index derived by the risk-based approach. Main conclusions are summarized in Table 6.

(1) $\boldsymbol{\beta_t > \beta_{l,opt}}$

Table 7 shows that the lifetime fatigue reliability β_L, structural investments C_{INT} and min life cycle costs C_L by the reliability-based approach, are all be higher than the risk-based approach. The min C_{INT} by the reliability-based approach is higher than the risk-based approach and thus is not minimum globally. When $\beta_t > \beta_{l,opt}$, stronger structural plans (a larger FDF and/or a shorter Δt_i) than the optimum plans derived by the risk-based approach is not more cost-beneficial; but to satisfy the constraint on β_t, the reliability-based approach would result in stronger structural plans than the risk-based approach.

Table 7: Optimum results by the risk-based and reliability-based HDM approaches ($\boldsymbol{\beta_t}$=3.5 and c_r/c_f=0.01)

	Risk-based HDM method	Reliability-based HDM method
$(FDF, \Delta t_i)_{opt}$	(6,15)	(5,10)
T (mm)	28.7	27.7
n	1	2
C_L	3540	4295
C_{INT}	3035	4107
β_L	3.025	3.532
C_D	1010	554.7
C_M	2025	3552.5

(2) $\boldsymbol{\beta_t < \beta_{l,opt}}$

Table 8 shows that the lifetime fatigue reliability β_L and structural investments C_{INT} by the risk-based approach are higher, but the life cycle costs C_L are lower. The min C_{INT} derived by the reliability-based approach is smaller than the risk-based approach and is minimum globally. When $\beta_t < \beta_{l,opt}$, the structural plans by the risk-based approach is stronger and the associated structural investments C_{INT} are higher than the reliability-based approach. The C_{INT} obtained by the risk-based approach is not minimum, but the higher C_{INT} is rewarded by greater reductions of failure risks, leading a lower C_L.

Table 8: Optimum results by the risk-based and reliability-based HDM approaches ($\boldsymbol{\beta_t}$=2.5 and c_r/c_f=0.001)

	Risk-based HDM method	Reliability-based HDM method
$(FDF, \Delta t_i)_{opt}$	(3,6)	(3,10)
T (mm)	25.0	25.0
n	4	2
C_L	823.5	1684
C_{INT}	775.8	573.5
β_L	3.679	2.775
C_D	125.0	125.0
C_M	650.8	448.5

(3) $\beta_t \cong \beta_{l,opt}$

When the β_t is approximately equal to (or slightly smaller than) the $\beta_{l,opt}$, the risk-based and reliability-based approaches could result in the same optimum plans, which is optimal in terms of both life cycle costs C_L and structural investments C_{INT} and satisfies the constraint of β_t. For example, when β_t=3.0 and c_{r0}/c_{f0}=0.01, the optimum structural plans by the risk-based (Table 3) and reliability-based (Table 5 (b)) approaches are the same. Note that the values of β_L, C_L and C_{INT} associated with the same structural plans, may not be identical in different tables (but are reasonably close), due to the random nature of the Monte Carlo simulations.

6.3.3 Sensitivity to the adopted inspection method

Table 9: Optimum results by the risk-based HDM Method (CVI)

	c_{r0}/c_{f0}	0.1	0.01	0.001	0.0001	0.00001
Risk-based design and maintenance holistic optimization	$(FDF, \Delta t_i)_{opt}$	(9,15)	(6,6)	(3,5)	(2,3)	(2,3)
	T (mm)	31.1	28.7	25.0	23.1	23.1
	n	1	2	5	9	9
	C_L	12974	3218	838.6	290.9	230.7
	C_{INT}	12518	2839	562.3	113.5	53.3
	β_L	3.056	3.112	3.203	3.329	3.329
	C_D	4356	1010	125.0	46.6	46.6
	C_M	8161	1829	437.3	66.9	6.7
	C_F	456.8	378.4	276.2	177.4	177.4

Table 10: Optimum results by the risk-based HDM Method (VI)

	c_{r0}/c_{f0}	0.1	0.01	0.001	0.0001	0.00001
Risk-based design and maintenance holistic optimization	$(FDF, \Delta t_i)_{opt}$	(9,10)	(6,6)	(4,2)	(4,2)	(4,2)
	T (mm)	31.1	28.7	26.5	26.5	26.5
	n	2	4	14	14	14
	C_L	12382	3139.7	1015.8	693	660.7
	C_{INT}	11983	2631.1	638.3	315.5	283.2
	β_L	3.096	3.023	3.112	3.112	3.112
	C_D	4356	1010	279.6	279.6	279.6
	C_M	7627	1621	358.7	35.9	3.6
	C_F	398.8	508.6	377.5	377.5	377.5

The optimum results by the risk-based HDM method using MPI, CVI and VI are given by Tables 3, 9 and 10 respectively. Based on the Tables, the following points are highlighted.

- The risk-based HDM method can result in different optimum fatigue designs when the inspection methods adopted at the operation stage are different, which cannot be achieved by fatigue design methods in which operational inspections are not considered quantitatively. For example, when c_{r0}/c_{f0}=0.00001 and MPI, CVI and VI is adopted respectively, the obtained optimum fatigue design factor is FDF=1, 2 and 4 respectively. This finding highlights the importance to explicitly consider the adopted inspection method at the fatigue design stage and make holistic decisions on structural scantling and operational maintenance.
- The obtained fatigue design factor generally becomes larger with a less accurate inspection method, which indicates that the obtained fatigue design factor is adaptive to the adopted inspection method.

A less accurate inspection method would lead to a less increase in reliability, so a larger fatigue design factor is derived by the method to achieve an optimum level of lifetime fatigue reliability.

- The derived optimum inspection interval generally becomes shorter when a less accurate inspection method is adopted. For example, when c_{r0}/c_{f0}=0.001 and MPI, CVI and VI is adopted respectively, the obtained inspection interval shortened from Δt_i=6 years (Table 3) to 5 years (Table 9) and to 2 years (Table 10). A less accurate inspection method leads to less increase in reliability, so more frequent inspections (i.e. shorter intervals) are obtained to achieve an optimum level of lifetime fatigue reliability. This finding shows the derived inspection interval is also adaptive to the adopted inspection method.
- The optimum inspection method is VI when c_{r0}/c_{f0}=0.1 or 0.01 and is MPI when c_{r0}/c_{f0}=0.001 or 0.0001 or 0.00001. These results are reasonable. When the ratio c_{r0}/c_{f0} is large, the costs of a repair are relatively high, and thus a less accurate inspection method (VI) is preferred which leads to lower expected maintenance costs. On the other hand, when the ratio c_{r0}/c_{f0} is small, failure costs are much higher than the costs of a repair, and thus a more accurate inspection method (MPI) is preferred which leads to more intensive maintenance and lower failure risks.

6.3.4 Sensitivity to the degree of uncertainty

Table 11: Optimum results by the risk-based HDM Method ($\mathbf{SD(\log_{10} C) = 0.14}$)

	c_{r0}/c_{f0}	0.1	0.01	0.001	0.0001	0.00001
Risk-based design and maintenance holistic optimization	$(FDF, \Delta t_i)_{opt}$	(8,15)	(6,15)	(4,6)	(2,3)	(2,2)
	T (mm)	30.4	28.7	26.5	23.1	23.1
	n	1	1	4	9	14
	C_L	20730	4141	885.4	172.0	61.2
	C_{INT}	20407	3056	855.3	158.9	60.5
	β_L	3.158	2.786	3.795	3.996	4.651
	C_D	2797	1010	279.6	46.6	46.6
	C_M	17610	2046	575.7	112.3	13.9
	C_F	322.9	1084	30.1	13.1	0.7

Table 11 shows that when the degree of uncertainty increases, the derived optimum structural plans by the risk-based HDM approach is either the same or become stronger.

- When c_{r0}/c_{f0}=0.1 or 0.01 or 0.0001, under the increased degree of uncertainty, the same optimum structural plans are obtained by the proposed method, but the lifetime fatigue reliability index β_L gets lower and the life cycle costs C_L become higher (due to a higher probability of detection & repair and thus higher maintenance costs C_M).
- When c_{r0}/c_{f0}=0.001 or 0.00001, under the increased degree of uncertainty, stronger optimum structural plans (a larger FDF and the same Δt_i) are derived by the proposed method, and the lifetime fatigue reliability index β_L is higher, but the life cycle costs C_L are also higher.

7 Conclusions

Cracks have been found common in large welded steel structures subjected to fatigue loads, e.g. ships and offshore structures. It is generally not realistic trying to prevent cracks from such structures only by structural design measures, due to challenges such as, a large number of fatigue-sensitive details, budget constraints, manufacture imperfections, the effects of aleatory and epistemic uncertainties, etc. Operational interventions (e.g. inspections and maintenance) are important for reducing the risk of losing structural integrity, identifying gross errors in design and fabrication, identifying over-loading and accidental damages, etc. A limitation in current practice is lack of connectivity in the decision-making on structural design measures and operational interventions. The effects of operational interventions are normally not quantitatively accounted for at the structural design stage. Inspections and maintenance plans are normally either based on experience or obtained by optimization at the operation stage. However, it is believed that it would be more beneficial to do risk assessment and informed maintenance optimization at the structural design stage when there is a higher degree of uncertainty and the impacts of decisions are greater.

This paper has developed a risk-based holistic decision-making (HDM) approach to optimum design and maintenance of fatigue-sensitive components. The approach envelopes major engineering decisions (structural scantling, operational inspections and maintenance) and several sources of uncertainty affecting the lifetime fatigue performance of structural details and supports holistic decision-making at the initial design stage. The integration of the below methods represents some extent of novelty:

1) Decisions variables in structural scantling and operational maintenance are holistically derived at the structural design stage by risk-based optimization. The method allows for effectiveness of both structural scantling and maintenance at an early stage, leading to effective utilization of the two risk mitigation measures, and optimum resource allocation between the structural design and operation stages.
2) The effects of uncertainties and expected cost consequences of failure are taken into account explicitly by probabilistic and risk modelling methods, which supports rational decision-making on structural scantling and maintenance plans towards a trade-off between safety and life cycle total costs.
3) The same decision basis for structural scantling and maintenance planning is established by developing a risk model based on probabilistic fracture mechanics (FM). Effects of both structural scantling and maintenance are measured under uncertainty using the model, benefiting coherent and connected decision-making on structural scantling and maintenance.

The approach and optimization problem have been formulated based on a repair effect model, probabilistic modelling of fatigue deterioration and inspection detectability, event tree analysis, reliability & risk calculations and life cycle cost analysis. Two alternative approaches have also been formulated for comparison purposes, i.e. risk-based separate decision-making (SDM) approach and reliability-based HDM approach. The three methods have been tested on a typical fatigue-sensitive detail in a ship structures, and the derived optimum structural (design and maintenance) plans have been evaluated via performance indicators (lifetime fatigue reliability, life cycle costs and structural investments). Sensitivities of the obtained structural plans and performance indicators to the cost ratio (i.e. relative costs of repair to failure), the adopted inspection method and the level of uncertainty have been studied in detail.

It has been shown that the proposed method yields structural plans associated with less life cycle costs than the comparison methods. The cost reductions are attributed to a holistic approach to life cycle structural decisions (i.e. structural design, inspection and maintenance). Specifically, the inclusion of maintenance optimization in the initial structural scantling optimization has facilitated intelligent decision-making and utilization of the two risk mitigation options adaptively to the cost ratio and achieved a best trade-off between design costs and maintenance costs. It is found that the advantage of the proposed approach is more obvious when the cost ratio is smaller. The approach has generated structural plans involving more maintenance interventions (i.e. a weaker design plan, and shorter inspection intervals) when the cost ratio is smaller, which has not been capable by the SDM approach. When the cost ratio is large, the derived structural plans by the proposed and the SDM approaches are almost the same. It is thus concluded that the method can yield combinations of structural design and maintenance plans, adaptively to the cost ratio, which are optimum in term of the least life cycle costs due to a best trade-off between design costs and maintenance costs.

It is also shown that the proposed approach can be used to determine the optimum level of lifetime fatigue reliability that should be targeted at by rational structural design and maintenance planning. This is evidenced by the finding that the approach generally yields structural plans associated with a higher lifetime fatigue reliability when the cost ratio is smaller (i.e. when failure consequences are higher), i.e. the obtained optimum lifetime fatigue reliability changes appropriately to failure consequences. This feature has been found in the results by the reliability-based HDM approach. Benefited from inclusion of expected costs of failure in the optimization formulation, the proposed approach realizes optimization of lifetime fatigue reliability and a best trade-off between safety and life cycle costs. In summary, the method achieves two trade-offs: a. between design costs and maintenance costs; b. between safety and life cycle total costs.

This paper has developed a risk-based holistic decision-making approach to optimal fatigue design, inspection and maintenance of one-component structural system (e.g. one fatigue-sensitive detail). It has been demonstrated that the method is able to quantify the combined benefits of design and maintenance measures to risk and cost reductions, and to yield fatigue design, inspection & maintenance plans and expected lifetime fatigue reliability that are optimum in terms of life cycle costs. The approach and conclusions lay foundation for developing optimum fatigue design, inspection and maintenance plans for multi-component systems. In future work, multi-component system level fatigue design, inspection and maintenance optimization would be addressed by taking into account dependencies among components. In addition, it is desirable to extend the approach by using more decision variables.

Acknowledgements

The authors would like to express their gratitude to the European Union's Horizon 2020 research and innovation programme for their funding toward this project under the Marie Sklodowska-Curie grant agreement No. 642453 (http://trussitn.eu).

References

[1] Soliman, M., D.M. Frangopol, and A. Mondoro, A probabilistic approach for optimizing inspection, monitoring, and maintenance actions against fatigue of critical ship details. Structural Safety, 2016. 60: p. 91-101.
[2] Lassen, T. and N. Recho, Fatigue Life Analyses of Welded Structures: Flaws. 2013: John Wiley & Sons.
[3] Moan, T., Life-cycle assessment of marine civil engineering structures. Structure and Infrastructure Engineering, 2011. 7(1-2): p. 11-32.
[4] Cui, W., F. Wang, and X. Huang, A unified fatigue life prediction method for marine structures. Marine Structures, 2011. 24(2): p. 153-181.
[5] Lassen, T. and N. Recho, Proposal for a more accurate physically based S– N curve for welded steel joints. International Journal of Fatigue, 2009. 31(1): p. 70-78.
[6] D'Angelo, L. and A. Nussbaumer, Estimation of fatigue SN curves of welded joints using advanced probabilistic approach. International Journal of Fatigue, 2017. 97: p. 98-113.
[7] DNV, G., DNVGL-RP-0005: Fatigue design of offshore steel structures. 2014, Det Norske Veritas AS, Oslo, Norway.
[8] Ayyub, B.M., et al., Reliability-based design guidelines for fatigue of ship structures. Naval engineers journal, 2002. 114(2): p. 113-138.
[9] Ayala-Uraga, E. and T. Moan, Fatigue reliability-based assessment of welded joints applying consistent fracture mechanics formulations. International Journal of Fatigue, 2007. 29(3): p. 444-456.
[10] Guedes Soares, C. and Y. Garbatov, Reliability of maintained ship hull girders subjected to corrosion and fatigue. Structural Safety, 1998. 20(3): p. 201-219.
[11] Chryssanthopoulos, M.K. and T.D. Righiniotis, Fatigue reliability of welded steel structures. Journal of Constructional Steel Research, 2006. 62(11): p. 1199-1209.

[12] Moan, T. and E. Ayala-Uraga, Reliability-based assessment of deteriorating ship structures operating in multiple sea loading climates. Reliability Engineering & System Safety, 2008. 93(3): p. 433-446.
[13] Moan, T. and R. Song, Implications of inspection updating on system fatigue reliability of offshore structures. Journal of Offshore Mechanics and Arctic Engineering, 2000. 122(3): p. 173-180.
[14] Chen, N.-Z., G. Wang, and C. Guedes Soares, Palmgren-Miner's rule and fracture mechanics-based inspection planning. Engineering Fracture Mechanics, 2011. 78(18): p. 3166-3182.
[15] Lotsberg, I., et al., Probabilistic methods for planning of inspection for fatigue cracks in offshore structures. Marine Structures, 2016. 46: p. 167-192.
[16] Zou, G., K. Banisoleiman, and A. González. Reliability-based inspection planning in view of both crack initiation and propagation. in 27th annual European Safety and Reliability Conference (ESREL 2017), Portoroz, Slovenia, June, 2017. 2017. CRC Press.
[17] Doshi, K., T. Roy, and Y.S. Parihar, Reliability based inspection planning using fracture mechanics based fatigue evaluations for ship structural details. Marine Structures, 2017. 54: p. 1-22.
[18] Straub, D. and M.H. Faber, Risk based inspection planning for structural systems. Structural safety, 2005. 27(4): p. 335-355.
[19] Faber, M.H., D. Straub, and J. Goyet, Unified approach to risk-based inspection planning for offshore production facilities. Journal of Offshore Mechanics and Arctic Engineering, 2003. 125(2): p. 126-131.
[20] Kim, S., M. Soliman, and D.M. Frangopol, Generalized Probabilistic Framework for Optimum Inspection and Maintenance Planning. Journal of Structural Engineering, 2013. 139(3): p. 435-447.
[21] Valdebenito, M.A. and G.I. Schuëller, Design of maintenance schedules for fatigue-prone metallic components using reliability-based optimization. Computer Methods in Applied Mechanics and Engineering, 2010. 199(33): p. 2305-2318.
[22] Gomes, W.J. and A.T. Beck, Optimal inspection and design of onshore pipelines under external corrosion process. Structural Safety, 2014. 47: p. 48-58.
[23] Gao, Z. and T. Moan, Fatigue damage induced by nonGaussian bimodal wave loading in mooring lines. Applied Ocean Research, 2007. 29(1-2): p. 45-54.
[24] Moan, T., Z. Gao, and E. Ayala-Uraga, Uncertainty of wave-induced response of marine structures due to long-term variation of extratropical wave conditions. Marine Structures, 2005. 18(4): p. 359-382.
[25] Kvittem, M.I. and T. Moan, Time domain analysis procedures for fatigue assessment of a semi-submersible wind turbine. Marine Structures, 2015. 40: p. 38-59.
[26] Wirsching, P.H. and Y.-N. Chen, Considerations of probability-based fatigue design for marine structures. Marine Structures, 1988. 1(1): p. 23-45.
[27] Soares, C.G. and T. Moan, Model uncertainty in the long-term distribution of wave-induced bending moments for fatigue design of ship structures. Marine Structures, 1991. 4(4): p. 295-315.
[28] Miner, M., Cumulative Damage in Fatigue Journal of Applied Mechanics 12 (1945) No. 3, pp. A159-A164, 1945.
[29] Xiong, J. and R.A. Shenoi, A durability model incorporating safe life methodology and damage tolerance approach to assess first inspection and maintenance period for structures. Reliability Engineering & System Safety, 2009. 94(8): p. 1251-1258.
[30] Sun, Q., H.-N. Dui, and X.-L. Fan, A statistically consistent fatigue damage model based on Miner's rule. International Journal of Fatigue, 2014. 69: p. 16-21.
[31] Pavlou, D.G., The theory of the SN fatigue damage envelope: generalization of linear, double-linear, and non-linear fatigue damage models. International Journal of Fatigue, 2018. 110: p. 204-214.
[32] Thompson, I., Fatigue damage variation within a class of naval ships. Ocean Engineering, 2018. 165: p. 123-130.
[33] Shetty, N.K., Probabilistic fatigue assessment of welded joints, in Probabilistic methods for structural design. 1997, Springer. p. 85-111.

[34] Dong, Y. and D.M. Frangopol, Incorporation of risk and updating in inspection of fatigue-sensitive details of ship structures. INTERNATIONAL JOURNAL OF FATIGUE, 2016. 82: p. 676-688.
[35] Paris, P. and F. Erdogan, A critical analysis of crack propagation laws. Journal of basic engineering, 1963. 85(4): p. 528-533.
[36] British Standard, B., 7910. Guide on methods for assessing the acceptability of flaws in metallic structures, 2005.
[37] Ang, A.-S., Life-cycle considerations in risk-informed decisions for design of civil infrastructures. Structure and Infrastructure Engineering, 2011. 7(1-2): p. 3-9.
[38] Darcis, P., et al. A fracture mechanics approach for the crack growth in welded joints with reference to BS 7910. in ECF15, Stockolm 2004. 2013.
[39] Lotsberg, I. and M.M. Salama, Crack propagation versus crack initiation lives of FPSO weld details. Threshold, 2010. 1000: p. 3.0.
[40] Moës, N., J. Dolbow, and T. Belytschko, A finite element method for crack growth without remeshing. International journal for numerical methods in engineering, 1999. 46(1): p. 131-150.
[41] Han, Q., et al., Determination of stress intensity factor for mode I fatigue crack based on finite element analysis. Engineering Fracture Mechanics, 2015. 138: p. 118-126.
[42] King, R., A review of fatigue crack growth rates in air and seawater. 1998: Health and Safety Executive Norwich, UK.
[43] Straub, D., Generic approaches to risk based inspection planning for steel structures. Vol. 284. 2004: vdf Hochschulverlag AG.
[44] Ghosn, M., et al., Reliability-based performance indicators for structural members. Journal of Structural Engineering, 2016. 142(9): p. F4016002.
[45] Kim, S. and D.M. Frangopol, Optimum inspection planning for minimizing fatigue damage detection delay of ship hull structures. International Journal of Fatigue, 2011. 33(3): p. 448-459.
[46] DNVGL, Probabilistic methods for inspection planning for fatigue cracks in offshore structures, DNVGL, Editor. 2015. p. 263.
[47] Elber, W., The significance of fatigue crack closure, in Damage tolerance in aircraft structures. 1971, ASTM International.
[48] Souza, G. and B. Ayyub, Probabilistic fatigue life prediction for ship structures using fracture mechanics. Naval engineers journal, 2000. 112(4): p. 375-397.
[49] Madsen, H., R. Torhaug, and E. Cramer. Probability-based cost benefit analysis of fatigue design, inspection and maintenance. in Marine structural inspection, maintenance and monitoring symposium. 1991.
[50] Zou, G., K. Banisoleiman, and A. González. Uncertainty quantification and calibration of a modified fracture mechanics model for reliability-based inspection planning. in 12th International Conference on Structural Safety & Reliability (ICOSSAR 2017), Vienna, Austria, August, 2017. 2017. ICOSSAR.
[51] Georgiou, G.A., PoD curves, their derivation, applications and limitations. Insight-Non-Destructive Testing and Condition Monitoring, 2007. 49(7): p. 409-414.
[52] Wall, M., S. Burch, and J. Lilley, Review of models and simulators for NDT reliability (POD). Insight-Non-Destructive Testing and Condition Monitoring, 2009. 51(11): p. 612-619.
[53] Garbatov, Y. and C.G. Soares, Cost and reliability based strategies for fatigue maintenance planning of floating structures. Reliability Engineering & System Safety, 2001. 73(3): p. 293-301.
[54] Eltaief, M., et al., Dynamic approach for optimal inspection planning of fatigue cracked components. Journal of Constructional Steel Research, 2015. 115: p. 263-275.
[55] Huynh, K.T., A. Grall, and C. Bérenguer, Assessment of diagnostic and prognostic condition indices for efficient and robust maintenance decision-making of systems subject to stress corrosion cracking. Reliability Engineering & System Safety, 2017. 159: p. 237-254.
[56] Kulkarni, S.S. and J.D. Achenbach, Optimization of inspection schedule for a surface-breaking crack subject to fatigue loading. Probabilistic Engineering Mechanics, 2007. 22(4): p. 301-312.

[57] Sheils, E., et al., Development of a two-stage inspection process for the assessment of deteriorating infrastructure. Reliability Engineering & System Safety, 2010. 95(3): p. 182-194.
[58] Zitrou, A., T. Bedford, and A. Daneshkhah, Robustness of maintenance decisions: Uncertainty modelling and value of information. Reliability Engineering & System Safety, 2013. 120: p. 60-71.
[59] Zhou, X., L. Xi, and J. Lee, Reliability-centered predictive maintenance scheduling for a continuously monitored system subject to degradation. Reliability Engineering & System Safety, 2007. 92(4): p. 530-534.
[60] Zhang, M., O. Gaudoin, and M. Xie, Degradation-based maintenance decision using stochastic filtering for systems under imperfect maintenance. European Journal of Operational Research, 2015. 245(2): p. 531-541.
[61] Huynh, K.T., et al., Modeling age-based maintenance strategies with minimal repairs for systems subject to competing failure modes due to degradation and shocks. European journal of operational research, 2012. 218(1): p. 140-151.
[62] Badía, F.G., et al., Optimal replacement policy under a general failure and repair model: Minimal versus worse than old repair. Reliability Engineering & System Safety, 2018. 180: p. 362-372.
[63] Aven, T. and U. Jensen, A general minimal repair model. Journal of Applied Probability, 2000. 37(1): p. 187-197.
[64] Wu, F., S.A. Niknam, and J.E. Kobza, A cost effective degradation-based maintenance strategy under imperfect repair. Reliability Engineering & System Safety, 2015. 144: p. 234-243.
[65] Van, P.D. and C. Bérenguer, Condition-based maintenance with imperfect preventive repairs for a deteriorating production system. Quality and Reliability Engineering International, 2012. 28(6): p. 624-633.
[66] Keprate, A. and R.C. Ratnayake, Probability of detection as a metric for quantifying NDE capability: the state of the art. The Journal of Pipeline Engineering, 2015. 14: p. 199-209.
[67] Wirdelius, H. and G. Persson, Simulation based validation of the detection capacity of an ultrasonic inspection procedure. International Journal of Fatigue, 2012. 41: p. 23-29.
[68] Rentala, V.K., P. Mylavarapu, and J.P. Gautam, Issues in estimating probability of detection of NDT techniques–A model assisted approach. Ultrasonics, 2018. 87: p. 59-70.
[69] Ali, M.S.S.A., et al., Bayesian synthesis for simulation-based generation of probability of detection (PoD) curves. Ultrasonics, 2018. 84: p. 210-222.
[70] Lassen, T. and N. Recho. Risk based inspection planning for fatigue damage in offshore steel structures. in ASME 2015 34th International Conference on Ocean, Offshore and Arctic Engineering. 2015. American Society of Mechanical Engineers.
[71] Moan, T., et al. In-service observations of cracks in north sea jackets. a study on initial crack depth and pod values. in PROCEEDINGS OF THE INTERNATIONAL CONFERENCE ON OFFSHORE MECHANICS AND ARCTIC ENGINEERING. 1997. AMERICAN SOCIETY OF MECHANICAL ENGINEERS.
[72] Beaurepaire, P., et al., Reliability-based optimization of maintenance scheduling of mechanical components under fatigue. Computer Methods in Applied Mechanics and Engineering, 2012. 221-222: p. 24-40.
[73] Zio, E. and M. Compare, Evaluating maintenance policies by quantitative modeling and analysis. Reliability Engineering & System Safety, 2013. 109: p. 53-65.
[74] Scarf, P.A., W. Wang, and P.J. Laycock, A stochastic model of crack growth under periodic inspections. Reliability Engineering & System Safety, 1996. 51(3): p. 331-339.
[75] Mendes, A.A., D.W. Coit, and J.L.D. Ribeiro, Establishment of the optimal time interval between periodic inspections for redundant systems. Reliability Engineering & System Safety, 2014. 131: p. 148-165.
[76] Cronvall, O., et al., A study on the effect of flaw detection probability assumptions on risk reduction achieved by non-destructive inspection. Reliability Engineering & System Safety, 2012. 105: p. 90-96.
[77] Zou, G., et al. A Probabilistic Approach for Joint Optimization of Fatigue Design, Inspection and Maintenance. in The 28th International Ocean and Polar Engineering Conference. 2018. International Society of Offshore and Polar Engineers.
[78] Tolentino, D. and S.E. Ruiz, Influence of structural deterioration over time on the optimal time interval for inspection and maintenance of structures. Engineering Structures, 2014. 61: p. 22-30.

[79] Kim, S. and D.M. Frangopol, Cost-based optimum scheduling of inspection and monitoring for fatigue-sensitive structures under uncertainty. Journal of Structural Engineering, 2010. 137(11): p. 1319-1331.
[80] Castaldo, P., D. Gino, and G. Mancini, Safety formats for non-linear finite element analysis of reinforced concrete structures: discussion, comparison and proposals. Engineering Structures, 2019. 193: p. 136-153.
[81] Castaldo, P., et al., Partial safety factor for resistance model uncertainties in 2D non-linear finite element analysis of reinforced concrete structures. Engineering Structures, 2018. 176: p. 746-762.
[82] Der Kiureghian, A. and O. Ditlevsen, Aleatory or epistemic? Does it matter? Structural safety, 2009. 31(2): p. 105-112.
[83] Gomes, W.J. and A.T. Beck, Optimal inspection planning and repair under random crack propagation. Engineering Structures, 2014. 69: p. 285-296.
[84] Mansour, A., Probability based ship design, implementation of design guidelines for ships: a demonstration. 1996: Ship Structure Committee, US Coast Guard.